January 2020

Design Of Spouted Fluidized Bed Computational Models For Advanced Energy Applications

Ryder Shallbetter

DESIGN OF SPOUTED FLUIDIZED BED COMPUTATIONAL MODELS FOR ADVANCED ENERGY APPLICATIONS

by

Ryder William Shallbetter
Bachelor of Science, University of North Dakota, 2016

A Thesis

Submitted to the Graduate Faculty

of the

University of North Dakota

in partial fulfillment of the requirements

for the degree of

Master of Science

Grand Forks, North Dakota
December
2020

Name: Ryder Shallbetter

Degree: Master of Science

This document, submitted in partial fulfillment of the requirements for the degree from the University of North Dakota, has been read by the Faculty Advisory Committee under whom the work has been done and is hereby approved.

DocuSigned by:
Gautham Krishnamoorthy
98BC25E78A1B4C8...
Gautham Krishnamoorthy

DocuSigned by:
Michael Mann
46F0545EE5FF405...
Michael Mann

DocuSigned by:
Steve Benson
E5C01DDA2CE74E6...
Steve Benson

This document is being submitted by the appointed advisory committee as having met all the requirements of the School of Graduate Studies at the University of North Dakota and is hereby approved.

DocuSigned by:
Chris Nelson
2E0AF068C733403...
Chris Nelson
Dean of the School of Graduate Studies

12/10/2020
Date

PERMISSION

Title Design of Spouted Fluidized Bed Computational Models for Advanced Energy Applications

Department Chemical Engineering

Degree Master of Science

In presenting this thesis in partial fulfillment of the requirements for a graduate degree from the University of North Dakota, I agree that the library of this University shall make it freely available for inspection. I further agree that permission for extensive copying for scholarly purposes may be granted by the professor who supervised my thesis work or, in his absence, by the chairperson of the department or the dean of the Graduate School. It is understood that any copying or publication or other use of this thesis or part thereof for financial gain shall not be allowed without my written permission. It is also understood that due recognition shall be given to me and to the University of North Dakota in any scholarly use which may be made of any material in my thesis.

Signature Ryder W. Shallbetter

Ryder W. Shallbetter

Date 12-17-2020

Table of Contents

LIST OF FIGURES

LIST OF TABLES

ACKNOWLEDGEMENTS

First of all, I would like to thank my wife, Nayana, for her love, support, and late nights that turned in to early mornings for me to achieve my goals. I have a deep and sincere gratitude towards her for making my success a priority.

Secondly, I would like to thank my advisor Dr. Gautham Krishnamoorthy for all of his guidance and help for the past seven years of undergraduate and graduate work.

I would like to thank all of my colleagues at the Institute for Energy Studies, Dr. Michael Mann for his patience, guidance, and advice he has provided, and Dr. Johannes Van der Watt for the weekend BBQ's to clear my head.

Finally, Dr. Steven Benson at Microbeam Technologies for his patient support and opportunities he has provided me to further my research.

ABSTRACT

Fluidization process technology has been widely studied since its first commercial uses during the 1920s. Initially, developmental progress was slow as fluidized beds are complex in design and often hard to scale up in size. However, with the emergence of computational fluid dynamics (CFD), researchers were able to simulate wide ranges of fluidization and create new fluidization designs to help solve complex problems. This study aims to determine if CFD can be effective in designing spout-fluid beds with draft tubes for advanced energy applications.

CFD has been employed for studying the fluidization characteristics, design and optimization of spouted beds. However, they have mainly been used in conjunction with large (Geldart D) particles where the drag forces dominate the wall frictional and collisional losses. Subsequently, identifying the correct drag law with the Geldart D particles has often deemed to be sufficient to get an accurate fluidization pattern. Additionally, the more accurate Discrete Element Method (DEM) methodology where the forces and motion of the individual particles are tracked has also been employed when the numbers of particles are computationally manageable (between 10^4 and 10^5). In this project the feasibility of employing Geldart B particles in spouted bed reactors are explored. In lieu of the fact that the number of resulting particles make the use of the DEM framework unfeasible we employ the Two Fluid Modeling (TFM) methodology in this scenario. Further, frictional and collisional losses become more important here (due to smaller particle sizes) which make the selection of appropriate interaction terms in the TFM framework all the more important.

The first CFD software used in this study was Multiphase Flow with Interphase eXchanges (MFiX), an open source CFD software created and maintained by the National Energy and Technology Laboratory (NETL). The purpose of using the MFiX software was to design a spout-fluid bed with a draft tube that may be used in Chemical Looping Combustion (CLC) applications with the goals of minimizing the pressure drop and maximizing the residence time. Specifically, the drag law, coordinate system, and grid/mesh resolution were studied to determine the optimal design settings. The optimal design settings were determined by comparing the simulation results to previous experimental work conducted.

For the drag law comparison, three commonly used drag laws (Syamlal-O'Brien, Gidaspow, Wen-Yu) in fluidized bed simulations were employed to select the law that give the optimal performance results in model. Results of the drag law comparisons showed that the Syamlal-O'Brien model (with appropriate parameters representative of the fluidizing particle) is the best drag law for the spouted fluid bed with draft tube. Therefore, it was employed in the comparisons of co-ordinate system and mesh resolution

The next parameter studied was the co-ordinate system set for the model. Due to the high computational cost associated with 3D simulations it is traditional to simulate the fluidization behavior using 2D axisymmetric grids or even 2D planar grids. While 2D axisymmetric grids are an accurate representation of a cylindrical reactor, the imposition of symmetric boundary condition along the axis can lead to unrealistic jetting behavior (which will be exacerbated in a spouted bed unit due to high centerline velocity). While many studies have shown that 2D planar and 2D axisymmetric result in similar fluidization characteristics in bubbling beds, the importance of this assumption in spouted bed units need to be ascertained. The results of our model showed that the

cylindrical 2-D axisymmetric simulation predictions were qualitatively similar to the fluidization behavior that was observed experimentally.

The final MFiX parameter studied was the grid/mesh resolution of the model. In bubbling beds, a cell size of 9 diameters has been deemed adequate to capture pressure drop. However, we need to ascertain if this is applicable in spouted beds with draft tubes. However, a comparison of pressure drop predictions from employing cell sizes of 11 particle diameters and 6 particle diameters showed that grid convergence was not yet achieved. Therefore, further research would be required to determine the optimal cell size for grid independence in spouted bed systems.

In the second part of this study, the CFD software ANSYS Fluent was utilized to determine the effectiveness of a spout-fluid bed with a draft tube for the density separation of particles. This specific design function may be desirable for the continuous removal of a product such as carbon black separation in the pyrolysis of tires. ANSYS Fluent was selected for this portion of the study due to its ability to handle complex geometry and enable the specification of phase-specific interaction terms (drag laws and collision models). The different particles investigated were of 300 and 100 μm diameters and 1200 and 4000 kg/m^3 densities respectively. The results of the CFD simulations showed that a stable spout-fluid bed with draft tube design could be created. However, no significant separation of particles was achieved.

Additionally, CFD simulations and experimental trials were conducted on conical bottom spouted beds to determine if separation of pyrite-rich minerals from coal. The results of the CFD and experiment both concluded that no separation was achievable. The recovery of coal product was only 5% of the original mass and the ash content of the product coal decreased to 25-28% when the target separation criteria was less than 20% ash. Therefore, we concluded for effective

density separation of Geldart B particles design modifications to the spouted bed reactor should be investigated in future work.

CHAPTER I

INTRODUCTION AND BACKGROUND

1.1 The Problem

The largest contributor to CO_2 emissions worldwide is from the use of fossil fuels in power generation. The most commonly fuel being used is coal which generates over 40% of the world's electricity (1). This high use of fossil fuels in worldwide energy production has led to a drastic increase in the global levels of carbon dioxide (CO_2) levels. Since 1980, the mean global annual mean atmospheric concentration of CO_2 has risen from 338.8 to 404.98 ppm in 2017, an increase of 20% (2). Experts have classified any CO_2 concentrations above 450 ppm or 1000 GtC (gram tons carbon) as catastrophic due to these high levels leading to warming of 3-4°C causing shifting the climate from the range at which humanity and other species are adapted (3). Therefore, reduction in CO_2 emissions is needed immediately as the current levels are only 11% away from this dangerous threshold. Reducing the emissions from coal plants can be achieved using several different technologies including fuel switching, efficiency improvements, and more recently carbon capture and storage (CCS).

1.2 Fuel-Switching

Fuel switching involves reconfiguring an existing power plant to operate with natural gas rather than coal as a fuel. Studies estimated that new power plants operating with natural gas will emit 50 to 60 percent less CO_2 then conventional coal plants (4). However, the methods used for

producing natural gas have potential harmful effects on the environment. Current research estimates that 2.3% of gross U.S. natural gas production is released into the atmosphere through

leakage. This amount of leakage causes changes to the climate similar to the CO2 from natural gas combustion over a 20-year time period (5). Therefore, methane losses must be kept at a minimum to reduce additional emissions while using the alternative fuel.

1.3 Increased Efficiency

Another technique industry has used to lower CO_2 emissions has been to improve the efficiency of coal plants. By increasing the efficiency of the plant, producers can decrease CO_2 emissions while maintaining optimal power generation. The overall efficiency of an existing plant can be achieved by upgrading the equipment to handle higher temperatures, improving combustion controls, and fuel upgrading. Currently the average efficiency of coal-fired power plants is 33% and improving the efficiency one percentage point would result in a 2-3% reduction in CO_2 emissions (6). Figure 1 below shows how improving the efficiency of various configurations of coal fired power plants would decrease efficiency.

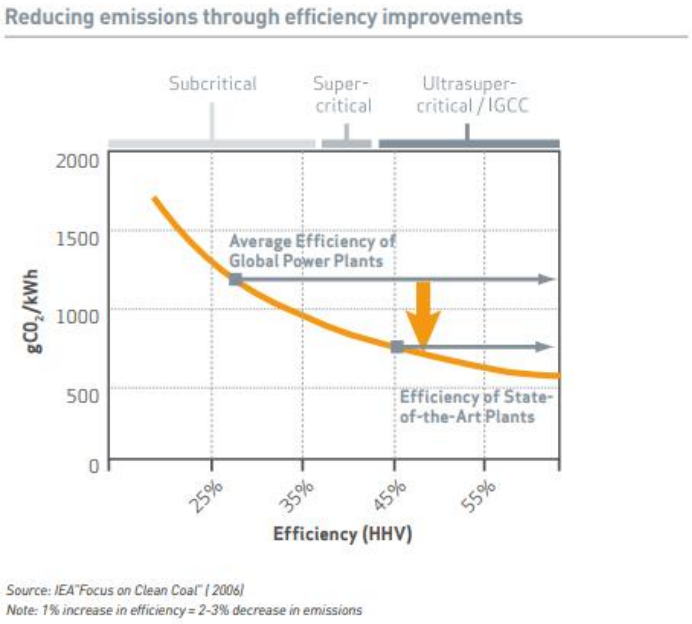

Figure 1. Impact of increasing the efficiency of coal-fired power plants on CO2 emission (7)

Notice the difference in emissions between the state-of-the-art plants and the global power plants. The new state-of-the-art plants have approximately 60% less CO_2 emissions and shown significantly reduced emissions of nitrogen oxides (NO_x), Sulphur dioxide (SO_2) and particulate matter (PM).

1.4 Carbon Capture Utilization and Storage

While fuel switching and efficiency improvement are each effective in reducing the overall CO_2 emissions, both technologies may be improved through the use of CCUS. The goal of CCUS technologies is to produce a near pure CO_2 product stream that can either be stored or used as a feed stock for a wide range of products. Currently, extensive research is underway to determine all the economical uses of the captured CO_2. The National Energy Technology Laboratory (NETL) are currently supporting a wide variety of projects dedicated to CCS technologies and produced Figure 2 below, displaying all the potential uses of captured CO_2.

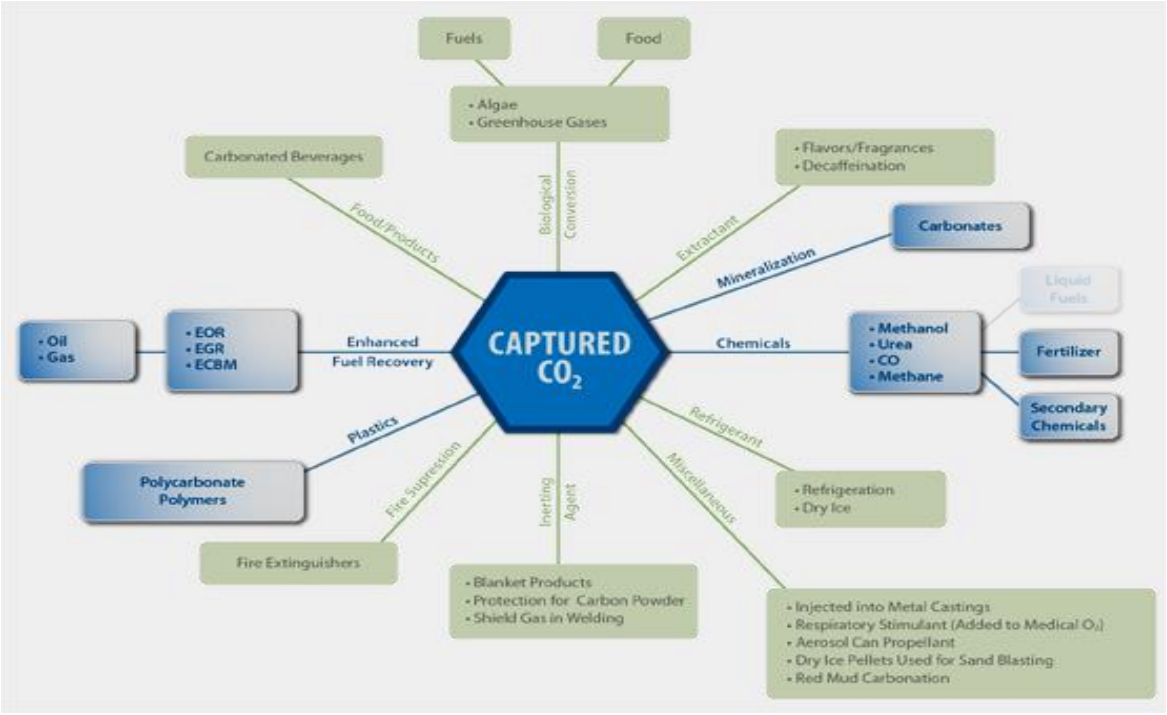

Figure 2. Potential uses for Captured CO2 with NETL focuses research in blue (8)

Three main technologies used to separate the CO_2 from produced gases include pre-combustion capture, post-combustion capture, and oxy-fuel combustion.

Pre-combustion capture is used when gasification is integrated into the power plant. The solid fuel is converted into a gaseous fuel known as syngas and used to fuel a turbine to produce electricity. The pre-combustion capture focuses on the syngas and removes the CO_2 by use of a solvent, sorbent, or membrane before the gas combusted in the turbine.

Post-combustion capture is employed to remove the CO_2 from the flue gas generated from the burning of the fossil fuel. In a typical coal-fired power plant, the coal is burned using air in a boiler to produce a high-pressure steam which drives a turbine to produce electricity. The produced flue gas is then treated to reduce the level of several harmful pollutants including NO_x, Sulphur dioxides, particulate matter, mercury, and finally CO_2. However, the removal of CO_2 is the most difficult due to the large quantity of nitrogen in the flue gas. Therefore, researchers have been looking into hybrid technologies combining solvents, sorbents, and membranes together to create the most efficient CO_2 capture.

Oxy-fuel combustion has also been researched for CO_2 capture applications. Oxy-fuel combustion power production operates by using an air separation unit (ASU) to remove the nitrogen (N_2) from the air before the combustion process. This results in the total volume of flue gas being produced to decrease by 75% compared to combustion using standard air. Furthermore, the lower flowrates of flue gas along with a high concentration of CO_2 (70% by volume) allow for an easier removal of CO_2 and other pollutants such as nitrogen oxides (NO_x), Sulphur dioxide (SO_2) and particulate matter (PM). However, the technologies used for oxy-combustion including cryogenic-ASU units are extremely costly and therefore are not commonly used in industry.

1.5 Chemical Looping Combustion

A new emerging CCUS technology that has seen rapid development is Chemical Looping Combustion (CLC). Like other CCUS technologies CLC focuses on generating a near-pure CO_2 product stream. However, unlike oxy-fuel combustion the oxygen is not obtained using an ASU. Instead, CLC using solid oxygen carriers (OC) to carry the oxygen to the fuel for the combustion process. Additionally, by using biomass or coal/biomass blends, capturing the CO_2 would greatly reduce the carbon footprint of the process and result in 'negative' carbon emissions.

1.5 Solution

Current CLC reactor configurations can meet the rigorous demands of CLC however they achieve these conditions with high operating costs and low system reliability. Therefore, there is a strong demand for configurations that can achieve the demands of CLC more effectively and efficiently. A spouted fluidized bed is a variation of a fluidized bed which due to its unique hydrodynamic features, are advantageous in the chemical looping process. Spouted fluidized beds in a CLC process can handle a wide range of fuels, and the configuration is modular and scalable which is critical for large-scale applications.

The performance of a spouted bed CLC reactor system is reliant on numerous variables including the gas velocities in the system, the reactor dimensions, and the physical properties of the fluids and solids within the system. Therefore, it is crucial to have a well-defined hydrodynamic model to accurately predict the sensitivity of the system to changes in the variables.

Hydrodynamic studies are essential to process development. A well-designed hydrodynamic model can allow the user to visualize conditions occurring in the reactor, rapidly conduct various what-if scenarios, and provide key assistance in the design process.

Figure 3 shows the generic process involved in the design process of hydrodynamic systems. Using data from process studies and hydrodynamic data on the system an initial model can be created. This model is then tested at the experimental level where data is collected for model verification. The updated model can then be used to scale-up the design and provide valuable insight to the design and operation of the system at a commercial scale. A well-defined model should evolve with the system over its entire lifecycle changing as new data is collected and analyzed to optimize the system.

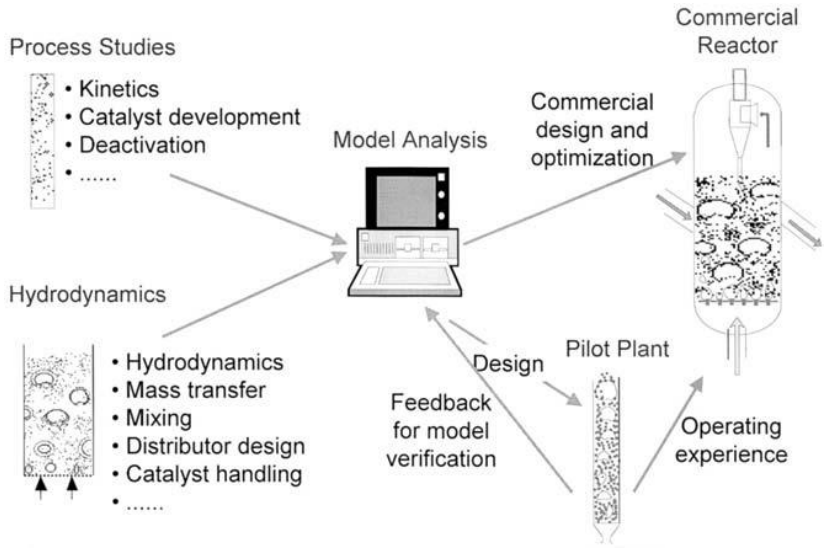

Figure 3. Hydrodynamic Modeling Design Process (9)

However, it is important to note that there are several limitations to hydrodynamic modeling that must be considered. There is a much-needed level of caution when interpreting the results from the simulations. The accuracy of the model may be limited due to insufficient data on the initial and boundary conditions and relative correlations. Therefore, trends predicted by the model are more valuable than the predict results. Another limitation is the complexity of the software for the user to create models and analyze their results. Often it takes several months to become an expert user. A final limitation is that hydrodynamic modeling requires significant

computational resources. However, this limitation has decreased over the past few years as technological advancements have made computers faster and more affordable.

1.6 Objective

This work focused on two main objectives. First, was to develop a computational modeling method for spouted fluidized beds with draft tubes for advanced energy applications such as chemical looping combustion (CLC).

To achieve this goal, MFiX was used to simulate the fluidized bed. MFiX is an open source code CFD solver with allows the simulation of complex hydrodynamic systems. Recently the interest in the MFiX technology has expanded rapidly. As seen in Figure 4 below the number of citations of MFiX has increased over 100x over the past 15 years.

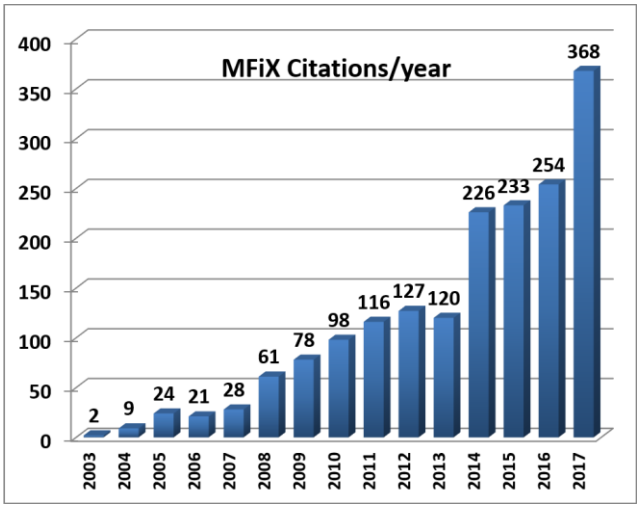

Figure 4. Number of Research Citations involving MFiX per year (10)

A robust and accurate modeling tool is essential as it provides rapid screening and optimization of the CLC process parameters. Furthermore, an accurate model allows for quicker time to market of CLC technology which have a potential impact to drastically reduce emissions. To satisfy the objectives of this work the following key questions were identified to be answered.

- What design aspects (spout diameter, spout and central jet velocities, draft tube location) of a spouted bed appear to be promising through CFD analysis for CLC system?
- Given the lack of information regarding the behavior of Geldart B particles in spouted bed reactors, which drag laws and models for the interaction terms are appropriate in these systems?
- Are there differences in fluidization characteristics, computational costs and accuracies in carrying out these simulations in Cartesian geometry and cylindrical co-ordinate systems
- What is the optimum mesh resolution to obtain grid independent predictions of pressure drop?

The second objective of this work was to apply the computational modeling methods learned from the CLC system and apply them to other advanced energy applications. It was chosen to study the application of density-based separation using a spouted bed with and without draft tubes. Previous studies of this application (11) that were conducted with conical spouted beds have shown success. By measuring weight fractions, they found that the dense particles concentrated in the upper section of the bed and near the spout while the lighter particles concentrated towards the walls. However, their studies focused on large particle systems with diameters between 1.5-3mm. We have chosen to study much lower particle diameters of 0.1-0.3 mm particle to determine if the same quality of separation may be achieved.

LITERATURE REVIEW

1.7 Fluidization and Fluidized Beds

Fluidization is the process of using a fluid, either a gas or liquid, where a bed of solid particles are suspended in a fluid-like state. At low flowrates, the fluid just merely passes through the bed of particles. As the flowrate increases the particles become fluidized when the frictional forces imposed by the fluid on the particle, known as the drag force, are significant to overcome the gravitational forces on the particle. When the drag force becomes equal to the weight of the particles in the bed, the bed is now considered to be at minimum fluidization. The flowrate of gas to achieve minimum fluidization is defined as the minimum fluidization velocity. The minimum fluidization velocity for spherical particles can be determined using mathematical relationships of the properties of the particle and the fluid. The most used equation is the Wen Yu equation.

After minimum-fluidization gas-solid and liquid-solid systems begin to behave differently. In liquid systems increasing flowrate past minimum fluidization results in a steady expansion of the bed with little instabilities. However, in gas-solid systems increasing flowrate past minimum fluidization leads to large instabilities within the bed.

Numerous factors in the systems affect the ease at which particles will fluidize and the operating conditions to sustain fluidization. These include the vessel geometry, gas inlet arrangement, type of solids, and the flow-type of the solids.

One main factor that will affect the ease of fluidization is the size and particle size distribution (PSD) of the solids in the system. In a fluidized bed, fine particles may agglomerate if they are full of moisture and therefore must be constantly broken apart for proper fluidization to occur. This may be achieved using a mechanical agitator or operating at higher gas velocity. However, fine particles that have a large PSD may be fluidized easily with large ranges of gas

flows allowing for design of deep, large, fluidized beds. Comparatively, large particles of similar sizes are difficult to fluidize properly and require a lower ranges of gas flows.

1.8 Fluidized Bed Configurations

The method of fluidization changes drastically as the inlet fluid velocity increases. Figure 5 below displays the various stages of fluidization that occur with increasing gas velocity.

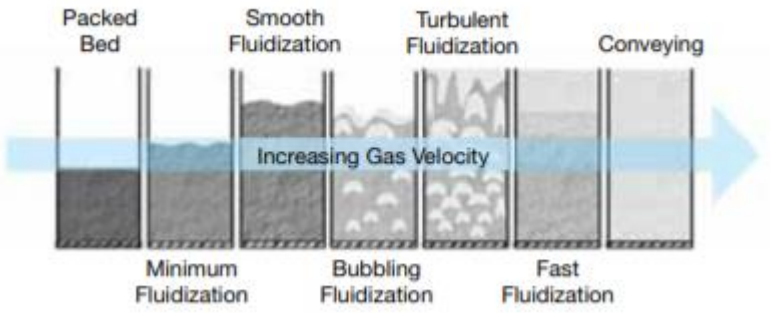

Figure 5. Various Methods of Fluidization (12)

When fluid is passed through the bed of particles at a low flowrate, the solids are not fluidized as the gas permeates through the bed and exits the reactor. This type of fluidized bed is known as a static or packed bed. As the gas velocity is increased, the bed will reach minimum fluidization and further increases will cause the bed to transition into a smooth fluidization. Next, the most common type of fluidized bed, the bubbling bed, may be observed. Further increasing the gas velocity will result in large instabilities in the bed as the gas bubbles expand rapidly throughout the bed. In certain cases of bubbling beds, if the bed has a large depth and small diameter the bubbles may expand across the vessel. This phenomenon is known as slugging. As gas velocity is increased even higher, fast fluidization occurs were the particles begin to become entrained out of the bed. Even higher velocities will result in the complete conveying of the solid particles through the system with no defined bed.

When a fluidized bed is designed for a new physical or chemical process, the method of contact between the fluid-solid is very crucial. Table 1 below gives a summary of process type versus the recommended fluidization scheme.

Table 1. Recommended fluidization configuration for processes

PROCESS	FLUIDIZATION CONFIGURATION
CATALYTIC REACTIONS	Fixed or Fluidized Beds
NON-CATALYTIC REACTIONS	Fluidized Beds
PHYSICAL OPERATIONS (HEATING, COOLING, DRYING OF SOLIDS, ADSORPTION OR DESORPTION OF VOLATILES)	Spouted Beds or Fluidized Beds

1.9 Fluidized Beds Advantages and Disadvantages

A Fluidized bed is generally more complicated to design, build, and operate compared to other industrial reactors such as packed-beds and stirred tank reactors. Table 2 shows a comparison of the advantages and disadvantages between the systems.

Table 2. Advantages and Disadvantages of Fluidized Beds

ADVANTAGES	DISADVANTAGES
-PARTICLE LIQUID-LIKE BEHAVIOR ALLOWS FOR STABLE OPERATION AND CONTROL	-High attrition rates leading to entrainment of particles in the gas that must be replaced
-NEAR ISOTHERMAL CONDITIONS HELP STABILIZE TEMPERATURE DURING EXOTHERMIC REACTIONS	-Higher levels of erosion on the bed surfaces due to the abrasive nature of the particles

-ABLE TO HANDLE LARGE-SCALE PROCESSES	-High mixing rates may lead to non-uniform residence times of particles
-HIGH HEAT AND MASS TRANSFER RATE BETWEEN PARTICLES AND GASES	

For the advantage of high heat transfer, fluidized beds can have a heat transfer rate of 5 to 10 times higher than a packed-bed system. The advantage of operating particles in a liquid-like behavior is essential when the process involves the use of a catalyst. Using a fluidized bed, the catalyst can be removed from the system without shutting down Furthermore, based on the configuration of the fluidized bed, the catalyst can be regenerated and recycled into the system. These types of configurations are called FCC or circulating fluidized bed reactor.

Fluidized beds however are not without their challenges. Due to the disadvantages listed in Table 2, fluidized beds are often difficult to scale-up in size. The high attrition and erosion mentioned also may result in the need for significant solid replacement which will increase the operating cost of the system.

1.10 Geldart Classification of Solids

The fluidization of gas-solid systems relies heavily on the type of solid used in the process. Geldart in 1973 was the pioneer in the classification of the behavior of solids in gas-solid systems. He characterized the behavior into four different groups defined by the density difference between the solid and the gas, and the mean particle size of the solid. The ranges of each of these classifications may be seen below in Figure 6.

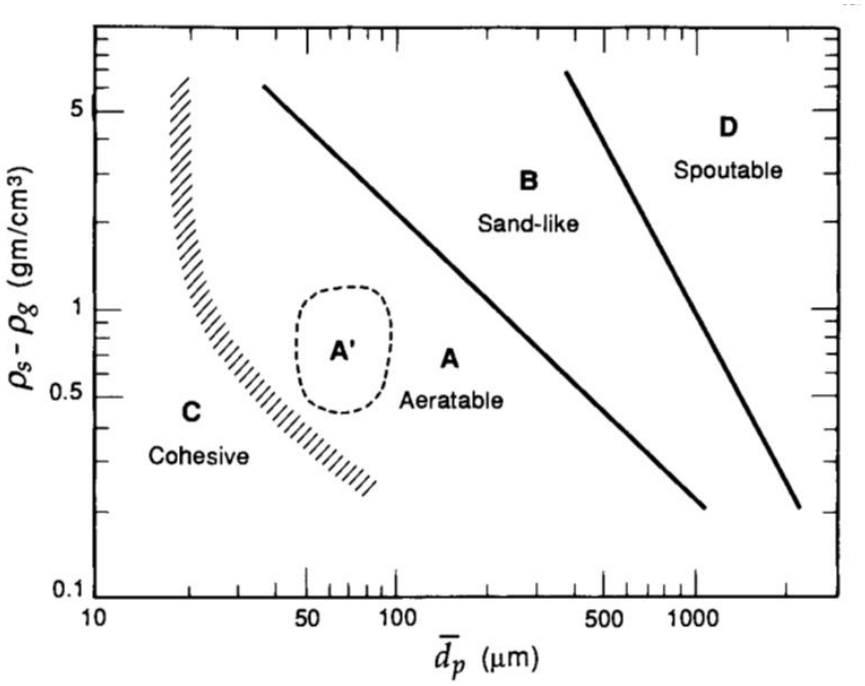

Figure 6. Geldart Classification of Solids (13)

Geldart's classification groups each have unique properties of the gas-solid fluidization. Particles in Group A, known also as aeratable, are very easy to fluidize and range from 30μm to 125 μm in size. At lower velocities smooth fluidization occurs and as velocity increases controlled bubbling with small bubbles will occur. However, when you have high bed pressures Geldart A particles may expand by 100% or more so additional design steps must be taken to prevent particle losses.

Particles in Group B are defined as sand-like particles, ranging in size from 150-1000 μm. These particles forgo smooth fluidization and fluidize well with vigorous bubbles that may grow large. Thus, their minimum fluidization velocity, and the minimum bubbling velocity, velocity required for bubbling to occur, are very similar. Due to their vigorous bubbling behavior, Geldart B particles are at a greater risk of forming slugging within the bed.

Group C particles are the smallest sized particles defined as cohesive. Fluidization is difficult to achieve with these particles are very "sticky" are hard to break apart. Because of their sticky nature, particle often behave as clusters rather than individual particles. Often channels form within the bed that allow for fast moving bubbles to bypass most of the bed of particles. Flour is a good example of a Group C particle.

Group D is comprised of large and or dense particles that are known as spoutable. Deep fluidized beds consisting of these particles are extremely difficult due to the large gas requirement to fluidize the particles. Therefore, Geldart D particles are most often used in a unique fluidized bed system called a spouted bed. Additionally, the particles behave erratically if the gas flow into the system is not uniform. Coffee beans and grains and peas are examples of Group D solids.

1.11 Mapping of Fluidization Schemes

To predict the behavior of fluidized bed systems it is important to know the contacting regime that will occur. The proper hydrodynamic expressions can then be selected for the regime. Grace (1) developed the first chart to map the various fluidization regimes. Later authors modified Grace's original chart with additional data and created a new chart, Figure 7. The chart utilizes the dimensionless forms of gas velocity u^* and particle diameter dp^*. Additionally, the

chart displays the lines for the minimum fluidization velocity and terminal velocity of the particles.

From the chart several key conclusions can be made. First, Geldart D particles are most associated with the spouted bed regime. Also, with Geldart D particles spouting can occur at gas velocities below minimum fluidization velocity. From the chart, bubbling beds can operate over a wide range of particle sizes from Geldart A to Geldart B. As the particle size increases the region for the bubbling bed regime decreases meaning the regime becomes harder to sustain. Furthermore, when particle size is decreasing, the bubbling bed regime region is increasing however it now requires flowrates above minimum fluidization velocity to achieve a stable bubbling bed.

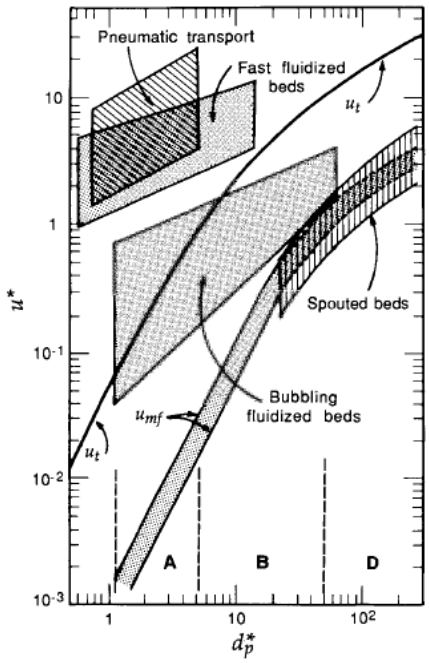

Figure 7. Flow regime diagram for various types of fluidization for the Geldart classification of solids adapted from Grace (15)

1.12 Spouted Bed History

The term spouted bed and spouting were first used by researchers Mathur and Gishler (16).The National Research Council (NRC) of Canada for the application of drying wheat. Mathur and Gishler were motived to develop spouted bed technologies to combat the limitations of fluidized beds. For fluidized bed technologies to be economically viable, the systems must utilize small particle sizes in the few hundred micrometers. Spouted beds may operate with much coarser particle sizes, a few millimeters, with the same effectiveness as fluidized beds. Their study investigated the effect of column diameter, fluid inlet diameter, bed depth, and the physical properties of solids and fluids on spouting behavior The publication of spouted bed research continued to originate from Canadian sources until 1959 when Max Leva wrote a book titled *Fluidization* (17). In his book he included a chapter which summarized the work the NRC and other Canadian researchers had accomplished. Research expanded next to research centers in the former Soviet Union once Leva's book was translated to Russian in 1961. The next major publication was *Spouted Bed* by Mathur and Epstein in 1974 which by this time over 200 publications had been written on spouted bed from all over the world. Later this collection was expanded on further by Epstein and Grace in 1997, *Spouted Bed and Spout-Fluid Beds*. Presently, there are over 3000 available publications, books, and patents on the conservative side.

Considerable research has been made into agricultural, chemical, pharmaceutical, and industrial applications for the technology. Specific uses that have been studied include converting agriculture waste streams such as rice husk and peanuts into energy through combustion, chemical looping combustion of coal, and dry premixing of sand and cement when producing mortar.

1.13 Spouted Bed Technology

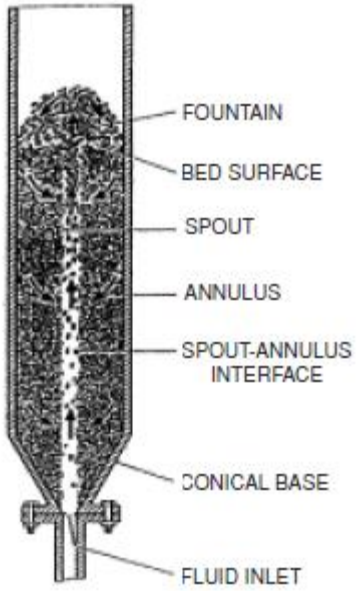

Figure 8. Schematic of spouted bed design with design labels (18)

In a spouted bed the fluidizing medium enters the bed through a small opening located centrally in the base of the vessel called the fluid inlet. The particles are then carried up the bed through central region called the spout before they splash, into the region above the bed called the fountain. Next, solids are circulated through a dense region outside of the bed called the annulus.

Important parameters that play a role in the formation of the spout within the bed are similar to those of fluidized beds. These parameters include the inlet flowrate, spout dimension, and the physical properties of the solids. Any change to these parameters may result in significant changes to the behavior of the bed and the spout. Therefore, spouted beds are not typically used for processes which involve critical control of the physical and chemical properties of the solids.

1.14 Spouting Versus Fluidization

As described in section 2.2 the Geldart classifications of solids has become the standard for determining the type of fluidization for various types of solids. From his work Geldart proposed a correlation to characterize the particles that can form stable spouted beds. Later in 1982, Molerus expanded further on Geldart's proposal. He derived a new criterion for particles that may form stable spouted beds. Molerus's correlation may be seen in Equation 1.

$$(\rho_p - \rho)gd_p > 15.3Pa \qquad (1)$$

Where:
ρ_p = density of the particle
ρ= density of the fluidizing medium
g = gravitational acceleration
d_p = density of the particle

Equation 1 emphasized the importance of a minimum particle diameter at which spouting becomes unstable and unreliable. However, Equation 1 was proven shown to be experimentally invalid by Chandnani and Epstein in 1986 (19).

The Geldart and Molerus equations failed to highlight the significance of the geometry of the reactor to promote spouting. An important design characteristic to achieve spouting in the bed is the ratio of the nozzle diameter to the column diameter, D_i/D. When this ratio is too high, the bed does not undergo spouting rather a rapid transition from a fixed bed into a fluidized state known as a pulsating bed. Additionally, another key ratio to promote spouting behavior is the nozzle-to-particle diameter ratio, D_i/d_p. Chandnani and Epstein (20) first reported the critical D_i/d_p ratio to be 25-30 to achieve stable spouting of fine particles.

Another defining characteristic of spouted beds over fluidized beds is the shape of the longitudinal profile of the bed. The geometry leads to a variance in the longitudinal pressure gradient in the bed when comparing spouted and fluidized beds. In a fluidized bed due to the uniformity of the profile the pressure gradient is constant while in spouted beds the pressure

gradient varies with height rising to a maximum value at the top of the bed. Studies have shown that the pressure drop across a spouted bed is lower by 20% than the pressure drop required for the full fluidization of the particles.

1.15 Spout-Fluid Beds

In 1970 Chatterjee (21) proposed a new type of bed called the spout fluidized bed or spout fluid bed. The spout-fluid bed is special hybrid bed that combines the characteristics of spouting and fluidized beds. These configurations are often used for coarse, sticky, or agglomerating solids. Spout-fluid reactors consist of a reactor with a single central office through which substantial fluid flow occurs, the spouting portion, while an additional flow of gas is provided through a distributor across the bottom of the reactor as in fluidized beds. When compared to spouted beds, spout-fluid beds have better gas-solid contact and mixing in the annular regions due to the additional flow from the distributor. Additionally, the total flow rate to fluidize the particles is lower than spouted beds and fluidized beds. Chatterjee supported this observation in his experiments sand particles in a cylindrical spouted bed. His results showed a 36% lower gas flowrate for the spout fluid bed compared to a conventional spouted bed. The distributor flow also helps to reduce the chances of particle agglomeration, dead zones, and particles becoming stuck to the walls of the reactor.

However, a downside of these improvements over the spouted is that spout-fluid beds are more hydro-dynamically complex. This complexity has led to challenges during the prediction of hydrodynamic properties within the beds in addition to scale up issues. Therefore, further experimental and theoretical work is necessary in order to develop accurate models to understand the validity of spout-fluid bed technologies.

1.16 Flow Regimes of Spout-Fluid Beds

A spout-fluid bed will have varying flow regimes depending on the gas flowrates through the central office and the distributor. Below in Figure 8 is a representation of the various flow regimes that may occur in a spout-fluid bed. Table 3 gives a description of each case.

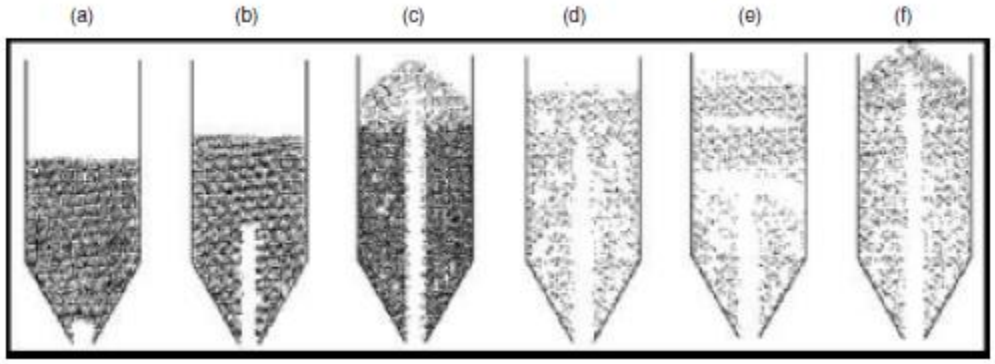

Figure 9. Various Flow Regimes of Spout-Fluid Beds (22)

Table 3. Description of various flow regimes in Figure 9

REGIME	NAME	DESCRIPTION
A	Fixed Bed	Particles are immobile as the gas flow is not large enough to fluidize the bed
B	Internal Jet	Gas flow is high enough to partially fluidize the bed, creating a submerged cavity or jet while the rest of the bed remains fixed
C	Spouting with aeration	Appearance of normal spouted bed, however is less stable due to bubbling at the bed surface
D	Jet Fluidized Bed with bubbling	Distinct jet with bubbling occurring at the top of the jet
E	Jet Fluidized Bed with slugging	Distinct jet with large bubbles forming in the middle and upper parts of the bed creating slugging
F	Spout-Fluidization	Upper section of the particles is fluidized leading to instability in the spout as bubbles discharge near the bed surface

Previous researchers have discovered that the flow regimes and transitions between them in a spout-fluid bed may be distinguished by analyzing the pressure fluctuation signals in the

bed. Methods suggested for analyzing the pressure fluctuations include power spectrum analysis (23) or Shannon entropy analysis (24).

1.16 Pressure Fluctuations in Spout-Fluid Beds

The pressure drop within the spout-fluid bed is dependent on the gas flowrate in both the spouting and fluidizing areas. Zhong and his colleges (25) studied the hydrodynamic characteristics of a spout-fluid bed pressure drop. First studied was the effect of changing the spouting gas velocity while keeping the fluidizing gas constant. They discovered as the spouting gas velocity increases, the pressure drop increases at first then decreases once a maximum value has been reached. As the velocity is increased further the pressure drop decreases suddenly to a smaller value and will remain fluctuating around this value as the velocity is increasing further. This phenomenon is identical to the behavior of spouted beds observed by Epstein and Grace (26). Therefore, it may be concluded that when increasing the spouting gas velocity while keeping the fluidizing gas velocity constant, the pressure drop of a spout-fluid bed is characteristic of a spouted bed. Additionally, Zhong tested the scenario of varying the fluidizing gas while keeping the spouting gas constant. They discovered that the pressure drop increases gradually with increasing gas velocity to a constant value which is similar to a fluidized bed. They also developed several correlations between the maximum pressure drop and operating conditions in the bed. It was determined that the maximum pressure drop required to initiate spouting increases with larger bed heights and particle density. However, the maximum pressure drop decreases with increasing particle diameter, spout nozzle width, and fluidizing gas velocity. These correlations are also observed in conventional spouted beds.

1.17 Applications of Spout-Fluid Beds

Research studies in the past have shown the wide variety of applications that the spout-fluid bed configuration has been applied to. At the University of British Columbia, researchers have been studied the use of spout-fluid beds for the combustion of low-grade solid fuels. They used three different bituminous coals or coal rejects with varying ash contents for the solid fuels. The goal of their research was to compare the throughput capacity and combustion efficiency of spouted and fluidized beds to that the results obtained using their spout-fluid bed. Initial results concluded that the spout-fluid bed yielded higher combustion efficiencies at low temperatures, with greater temperature uniformity, and an improved bed-to-surface heat transfer rate when compared to the other bed configurations (27).

Another application that spout-fluid bed technology was adapted for was use in the agricultural industry. Researchers at Mindanao Polytechnic State College of the Philippines studied the combustion of rice husks in spout-fluid beds (28). Their objective was to determine how varying the airflow rates, and method of feeding the fuel effected the emission of pollutants and feasibility of the rice husk fuel. It was discovered that spout-fluid beds can be used to convert agricultural residues into energy with the benefits of fuel flexibility, low emissions of pollutants, low operating temperatures, and isothermal operating conditions.

There has also been a significant amount of research for the use of spout-fluid bed for gasification processes. The Coal Research Establishment, part of the British Coal Corporation, developed a low-cost process technology which produces a low-calorific (4 MJ/m^3) fuel gas using a spout-fluid bed. (29). The produced gas is then integrated into an electricity generating system known as the British Coal Topping Cycle. The advantages of this system include improved thermal efficiency, reduced operating costs, and a lesser environmental impact.

1.18 Spout-Fluid Beds with Draft Tubes

The concept for spout-fluid beds with draft tubes was first described as a recirculating fluidized bed by Yang and Keairns (30). Other names for the technology that have been used include spouted fluid bed with a draft tube, circulating fluidized bed, or the internally circulating fluidized bed. By inserting in a draft tube, the fluid residence time and solid residence time in the bed can be controlled much easier. However, to reach this level of control the solid and fluid phase hydrodynamics in the bed are essential to know. Additional effects of inserting the draft tube into the bed include no bed height restriction for spouting and less gas leaking from the spouting inlet into the annular region compared to a typical spouted bed design.

Below in Figure 10 is the design of a typical spout-fluid bed with a draft tube. Gas enters the spout-fluid bed with a draft tube the same as a spout-fluid bed. The background or auxiliary gas will enter through the annular section while the spouting gas enters through the central spout. Spouting of the particles will occur as you vary the flowrates of each of the gases. If the auxiliary gas is held constant, specific behavior may be seen as the spouting-gas velocity is increased. At low spouting gas flowrates, the particles will form a small cavity above the spout-inlet with no particles in the draft tube. As you increase spouting flow, particles will start to become entrained from the annulus. Further increases will cause the particles to become fluidized in the draft tube and begin to expand up the draft tube. Then, at a critical spouting flowrate, called the minimum turnover velocity, particles will reach the top of the draft tube and spill out into the annular region.

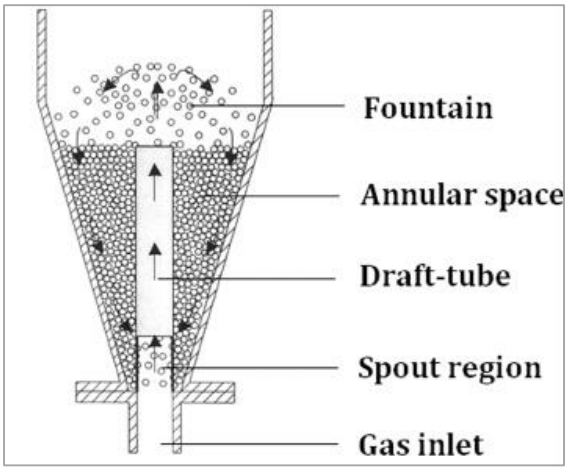

Figure 10. Spouted with draft tube bed configuration (31).

1.19 Spout-Fluid Beds with Draft Tubes Design

For the general design of a spout-fluid bed with draft tubes several design and operation parameters affect the hydrodynamics of the bed. These parameters include the inlet jet fluid flowrate, inlet auxiliary fluid flowrate, the internal annulus fluid flowrate, inlet section length, and the height of the annular region. Furthermore, the draft tube inlet length will affect the fluid leakage into the annular region from the central jet and the amount of solids crossflow occurring. Additionally, the auxiliary fluid flowrate will control the pressure drop across the bed and will alter the solids flow within the bed. Based upon the design of the bed the draft tube region may be characterized by two types of flow, draft tube operated as a fluidized bed and as a dilute phase pneumatic transport tube.

LaNauze in 1976, (32) proposed the first mathematical models for the condition of a draft tube operating as a fluidized bed. He discovered that the main driving force for solids circulation under his conditions was the density difference between the draft tube and the annulus. Additionally, LaNauze found that the solids circulation rate was only affected by the distance between the distributor and the draft tube and not the draft tube length or height of the bed. A disadvantage of operating the draft tube as a fluidized bed is related to the design of the draft

tube. If the diameter is too small or the tube is too tall then the draft tube will operate in a slugging mode.

1.20 Gas Bypassing Phenomenon

A common phenomenon that may occur in spout-fluid beds with draft tubes is gas bypassing the draft tube and flowing into the annular region. The various design and operating parameters of the spout-fluid beds makes it challenging to predict the distribution of the gaseous flow to the draft tube and annulus. Numerous studies have attempted to quantify the cause and effect of gas bypassing however no simple relationship exists, and no rigorous model has been proposed. Because no relationship exists, generally gas bypassing data is determined experiments on a case by case basis. General relationships that have been observed previously are that gas bypasses from the draft tube into the annulus at small draft tube to annulus area ratios. Additionally, it has been observed that gas will bypass exclusively from the annulus into the draft tube when the distance between the annular distributor and draft tube inlet is small.

1.21 Experimental Studies of Spout-Fluid Beds with Draft Tubes

In 1982 Grbavcic published an early investigation into basic properties of spout-fluid beds with draft tubes including minimum fluid flow, pressure drop, and the solid circulation rates. Grbavcic's work resulted in two main conclusions relating ratio of the height of the inlet section and the height of the bed. First, it was discovered that there is a minimum inlet section length below which no particle circulation from the annulus into the draft tube will occur. Secondly, a maximum value of the ratio exists at which pneumatic transport cannot occur in the draft tube due to gas bypassing into the annulus.

Additionally, Grbavcic (33) developed several relationships for the minimum spouting and annular flowrates required to initiate circulation in the draft tube. Grbavcic determined that

the solids mass flux will increase rapidly as the inlet section length increases while keeping the annular and spout flowrates constants. Also, he determined when increasing the annular gas flowrate will the spout flowrate is zero, the bed will expand as the velocity approaches the minimum fluidization velocity. Slightly increasing past the minimum fluidization velocity will cause particles to be entrained in the draft tube while the annulus remains un-fluidized. If the annular flowrate is increased substantially more, solid circulation can occur in the bed with the need for a spouting gas. Furthermore, he discovered that if the annular region extends to slightly below the top of the draft tube then the annulus region could not be fluidized.

1.22 Computational Fluid Dynamics

Computational Fluid Dynamics (CFD) modeling has become a powerful tool over the last several years for understanding multiphase flow. By using CFD, a range of flow properties may be estimated without any disturbance to the overall flow. Currently, there are two different methods of CFD modeling, the Eulerian-Lagrangian approach and the Eulerian-Eulerian approach.

The Eulerian-Lagrangian (discrete element method, DEM) method solves the Newtonian equations of motion for each individual particle within the system. It considers the collision effects from the non-ideal particle-particle interactions. The DEM method is used less likely as each individual particle is being tracked which leads to more computationally complex systems that require greater time for completion. Further, they cannot be used in this case due to the need to simulate a large number of particles ($10^4 – 10^5$).

The Eulerian-Eulerian (two-fluid model, TFM) method treats each of the phases continuous phases that are interpenetrating continua. The phases are overlapping with each phase having its own volume fraction which sum to 1. This method is more easily applied to multi-

phase flows which contain large volume fractions of solid phases. It is also often the default method to use for CFD as it takes significantly less computational resources than the DEM method.

1.23 CFD and Drag Laws

In CFD modeling, the drag force is the most important force acting on the particles in a gas-solid two-phase system. Numerous researchers have investigated the effects of the different drag-laws on CFD models. Dua (34) investigated the use of several widely used drag laws in CFD simulations of spouted beds. He concluded that the various drag laws caused significant differences between the simulations. In their case the Gidaspow drag law was the best fit for their experimental results.

Another researcher Gryczka (35) concluded that each drag law application is bound by a specific range of the particles Reynold's number. Furthermore, for his data there was better agreement when using the Schiller and Naumann model.

Each of these researchers determining different effective drag laws shows that there is not one universal drag law that can describe every possible fluidized bed configuration. Therefore, it is an important step whenever conducting CFD simulations to simulate multiple drag laws to ensure the correct model is chosen.

1.24 CFD of Spout-Fluid Beds with Draft Tubes

CFD simulation of spout-fluid beds with draft tubes have used both the DEM and TFM. Zhao (36) published a paper studying the motion of 2 mm diameter particles in a 2-D rectangular spouted bed with draft plates using DEM-CFD. His results gave accurate predictions of the longitudinal particle velocity profiles along the center of the bed and predicted no clustering of particles within the bed. In a contrasting report, Szafran and Kmiec (37) conducted CFD

simulations of 0.22, 1, 2.0, and 3.7 mm diameter particles and discovered particle clustering. The observed fluctuations in the spouting behavior of the bed caused by particle clusters at the base of the bed. This results in a slugging behavior of the bed with varying fountain height and porosity.

CHAPTER 2

SPOUTED FLUIDIZED BED WITH DRAFT TUBE

2.1 Previous Research

Previous experimental work at UND has been completed investigating the design of a spout-fluid bed with a draft tube for CLC systems (38). National Energy Technology Laboratories' CFD code MFiX (?) was used to create a hydrodynamic model of an existing reactor design seen in Figure 11.

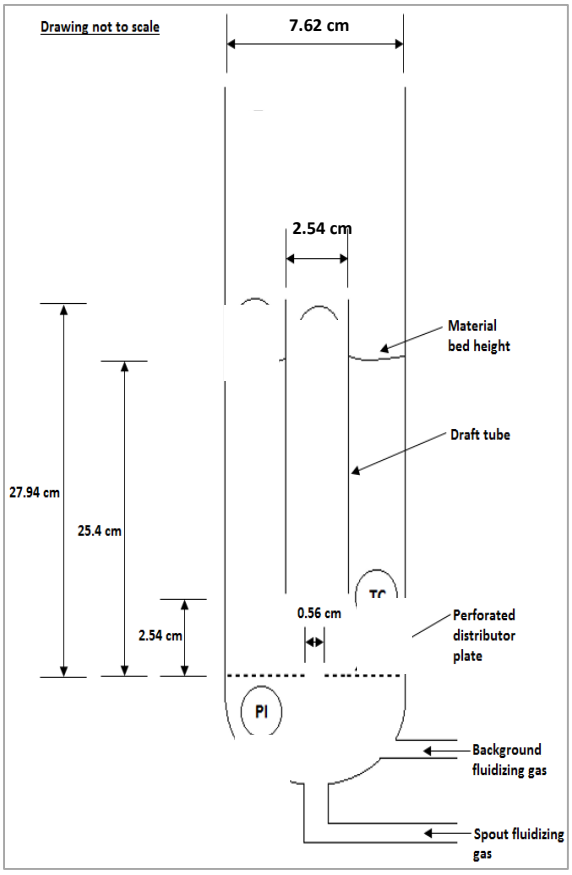

Figure 11. Geometry and dimensions of the spouted fluidized bed test system.

A cold-flow model was created to determine the effect that six design-variable may have on the spouting behavior of the bed, specially the material circulation rate. To determine the impact each variable had on the system, a fractional factorial design of 33 runs, was created using low- and high-level values from prior simulations. The levels for each of the factors are illustrated in Table 4.

Table 4. Fractional factorial design factors and values

Factor	Low Level Value	High Level Value
A: Bed height (cm)	15	30
B: Draft tube height from bottom (cm)	1	3
C: Draft tube internal diameter (cm)	2.6	4.6
D: Spout diameter (cm)	0.56	0.76
E: Spout velocity/Minimum fluidization velocity, Usp/Umf	95	142
F: Background velocity/Minimum fluidization velocity, Usp/Umf	0.5	1.25

The results from the fractional factorial design indicated that Factors B, C, and E influenced the material circulation rate the most. The high-level value of Factors B and E and the low-level factor of Factor C was determined to increase the overall material flowrate.

Once the key design factors were identified, a cold-flow laboratory fluidized bed reactor was manufactured to evaluate the validity of the MFiX model. Both the MFiX model and the laboratory experiments represented the spouting of the bed similarly; the spouting behavior displayed is not continuous but rather intermittent in nature. Intermittent spouting may be defined as: solid material building in the draft tube section then once enough force has been applied, the material exits the draft tube in a spout falling to the annular regions. Therefore, a

main conclusion from this work was that MFiX can accurately model a spouted fluidized bed system.

2.2 Technical and Experimental Approach

An overarching goal of this study is to establish a robust design/modeling framework that incorporates the necessary physical modeling elements to enable its utility in the design, scale-up and optimization of chemical looping in spouted fluid bed configurations. In the previous CLC spouted fluidized bed research at UND, it was established that MFiX could predict their behavior accurately. However, the previous work mainly focused on the physical dimensions of the reactor and the flowrates of inlet gases. The MFiX software is a complex modeling tool which allows for the specification of numerous hydrodynamic properties and computational settings. Therefore, in order to create a more robust modeling tool, the hydrodynamic and computational settings of the MFiX model were investigated further. For each MFiX model, the simulation was run for a simulation time of 30 seconds to allow the system to reach steady-state operation.

It is also important to note for all MFiX simulations in this study the MFiX-TFM (two-fluid model) was utilized. For more information on the governing equations of the model please refer to the Theoretical Review of the MFIX Fluid and Two-Fluid Models (39).

One setting that was investigated was the drag law specified for the model. MFiX allows the user to specify the gas-solid drag model from literature or the user may define their own custom drag law. In this study three different drag laws were studied, Syamlal-O'Brien with C1 D1 defined, Gidaspow, and Wen-Yu. The parameters C1 and D1 for the Syamlal-O'Brien drag law are tuning parameters that may be calculated using a spreadsheet available on the MFiX website (40).

Another setting investigated in this study was the coordinate system of the model. MFiX has two types of coordinates available for simulations, Cartesian and cylindrical. To determine the impact that changing the coordinate system would have on the simulation, the same drag law, Syamlal-O'Brien C1 D1, was used when varying the coordinate system.

The final MFiX setting that was studied was the grid sensitivity or mesh size of the model. All the MFiX models were restricted to 2-D geometries therefore only the number of cells in the x and y direction could be altered. However, only the effect of varying the number of cells in the x-direction was studied. Between the cases, the drag law and coordinate system remained constant, Syamlal-O'Brien C1 D1 and cylindrical, to solely determine the effects of grid size.

To determine the effect of changing the MFiX simulation parameters, a comparison variable must be determined. Within fluidized bed systems one of the most important measurements to record is the pressure. By analyzing changes in the bed's pressure, it is possible to define the behavior of the bed. In our comparisons, the pressure in the bed was monitored in the region between the spout and the entry into the draft tube. This region was chosen because during steady-state operation, the pressure in this region should remain constant. For each simulation, the average pressure was calculated for the region, during the simulation time of 5-25 seconds. The resulting average pressures for each simulation were then compared to determine the effects of changing the parameters.

Additionally, the physical behavior of the bed in each simulation may be visualized by examining the gas void fractions at various simulation times. This will provide insight into the effects of changing the MFiX parameters that may not be directly evident from the pressure results.

The spout-fluid bed reactor design used in this study is the same design used in the previous work at UND. From the previous work's results, the model employed in this study used

the factor settings that achieved a high material circulation rate. A summary of the important reactor design-variables may be seen below in Table 5. Additionally, the significant input variables for the MFiX model may be seen in Table 6.

Table 5. Important Design Variables for MFiX model

Design Variable	Value	Unit
Reactor Diameter	7.6	cm
Spout Diameter	0.56	cm
Draft tube internal diameter	2.6	cm
Draft tube height from bottom	3	cm
Bed Height	30	cm
Spout velocity/Minimum fluidization velocity, Usp/Umf	142	
Background velocity/Minimum fluidization velocity, Ubg/Umf	0.5	

Table 6. Significant input variables for MFiX model

Input Variable	Value
Particle Size	289 μm
Particle Density	4 g/cm^3
Fluidizing gas	Ambient air
Restitution coefficient	0.8
Friction coefficient	30°
Gas void fraction at minimum fluidization	0.44

2.3 Drag Law Comparison

The MFiX parameter first investigated was the drag law defined for the simulation. In the previous MFiX work completed by UND, the default drag law Syamlal-O'Brien C1 D1 was the only one studied. The default drag law plus two new drag laws were introduced to determine what effects they would have on the behavior of the bed. For each drag-law all other MFiX settings remained constant with the geometry set as cylindrical. The result of the average pressure for each drag law over the 5-25 second simulation time may be observed in Figure 12 below. Data analysis

begins after the 5 second mark to allow the bed to reach a steady state operation. In the figure the Wen-Yu drag law was omitted as the simulation failed after 10 seconds of simulation time.

Because there is no experimental data to compare the simulation to, the ideal drag law for the model is the drag law that provides the model with stability. Stability defined in our model would be consistent average pressure readings which would a stable spout and operation in the bed.

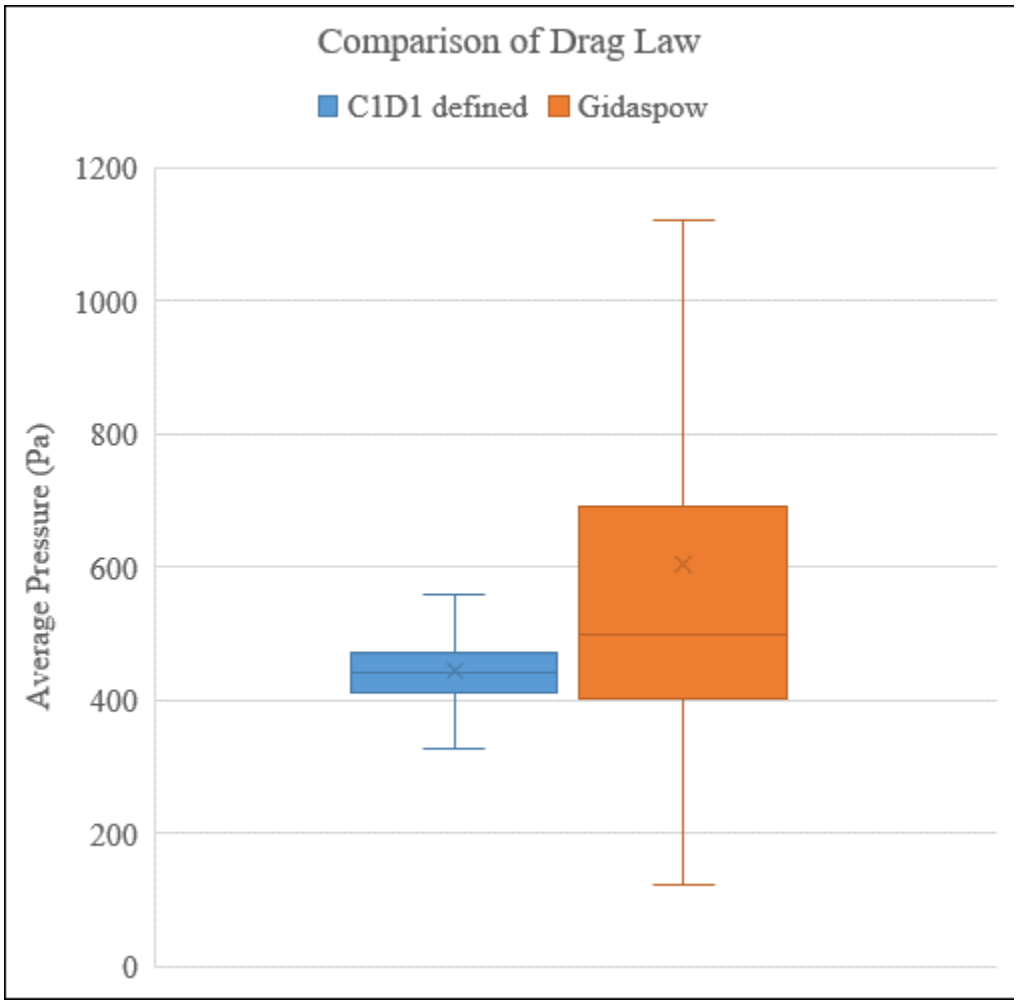

Figure 12. Comparison of average pressure in different drag law simulations

Interpreting the results of the figure above, it may be concluded that the Syamlal-O'Brien C1 D1 drag law is the more stable drag law for our model. This was an expected result as it is the default drag-law for the MFiX software. The Gidaspow model predicted a higher average pressure indicting a stronger spout flow however the model also showed a larger variance in the pressure. In addition, the Gidaspow simulation failed around the 25 second simulation time.

To understand why the deviations in the pressure reading are occurring, we can examine the gas void fraction of the bed at various time-steps. The behavior of the bed with each drag law may be seen in Figures 13-14 with a 5 second lapse between each. In each of the time steps the EP_g is equal to the void fraction of the gas phase.

After 5 seconds of elapsed simulation both the drag laws are showing the same behavior of intermittent spouting through the draft tube. In both the C1 D1 and Gidaspow cases you can see material that is spouting out of the top of the draft tube. The C1 D1 is spouting and breaking just barely above the top of the draft tube while the Gidaspow shows a separation between the spout and top of the draft tube. This agrees with the conclusion from the average pressure data that the Gidaspow model would show greater spouting strength.

At the 10 second mark the Wen-Yu model predicted that the gas void fraction is almost 1 throughout the entire bed implying the solids had blown-out of the bed. This led to the exclusion of the Wen-Yu drag law from the pressure comparison and void fraction visualization as not enough data was available and also lead to the conclusion that it is not the optimal drag-law. Both the C1 D1 and Gidaspow drag laws are still showing stable spouting behavior currently.

Next, after 15 seconds of elapsed simulation time it is observed that on the Gidaspow model there is a small fraction of solids in the gas on the sides of the reactor above the bed. This represents

that there may be some gas bypassing occurring into the annulus section. At this time step, the C1 D1 model is still showing stable flow of solids through the spout region.

At 20 seconds both the C1 D1 and Gidaspow models show stable operation. However, at the 25 second mark the Gidaspow model now displays clear signs of gas bypassing into the annulus as the spout region is clear of solids and the solids in the annular region being forced to the walls of the reactor.

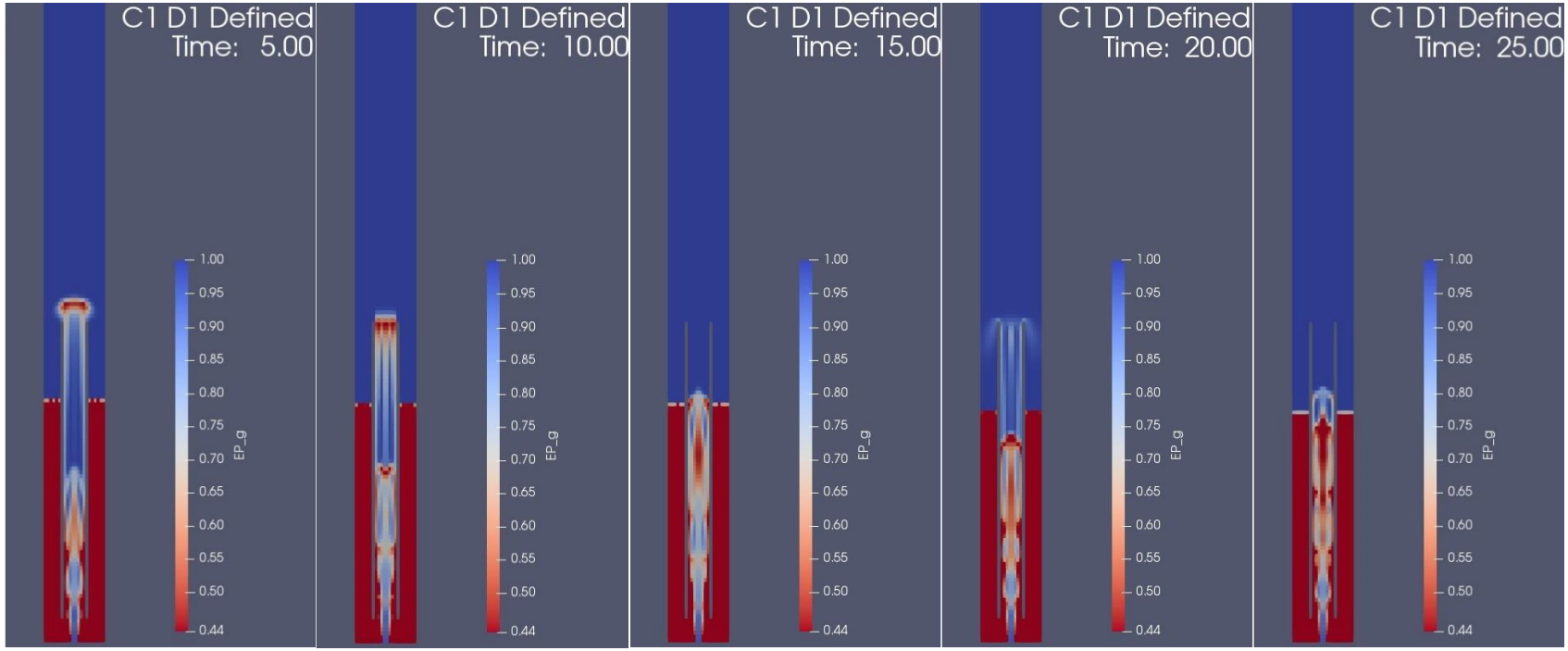

Figure 13. Syamlal O'Brien C1 D1 drag law gas void fractions at 5 sec incremental elapsed simulation time

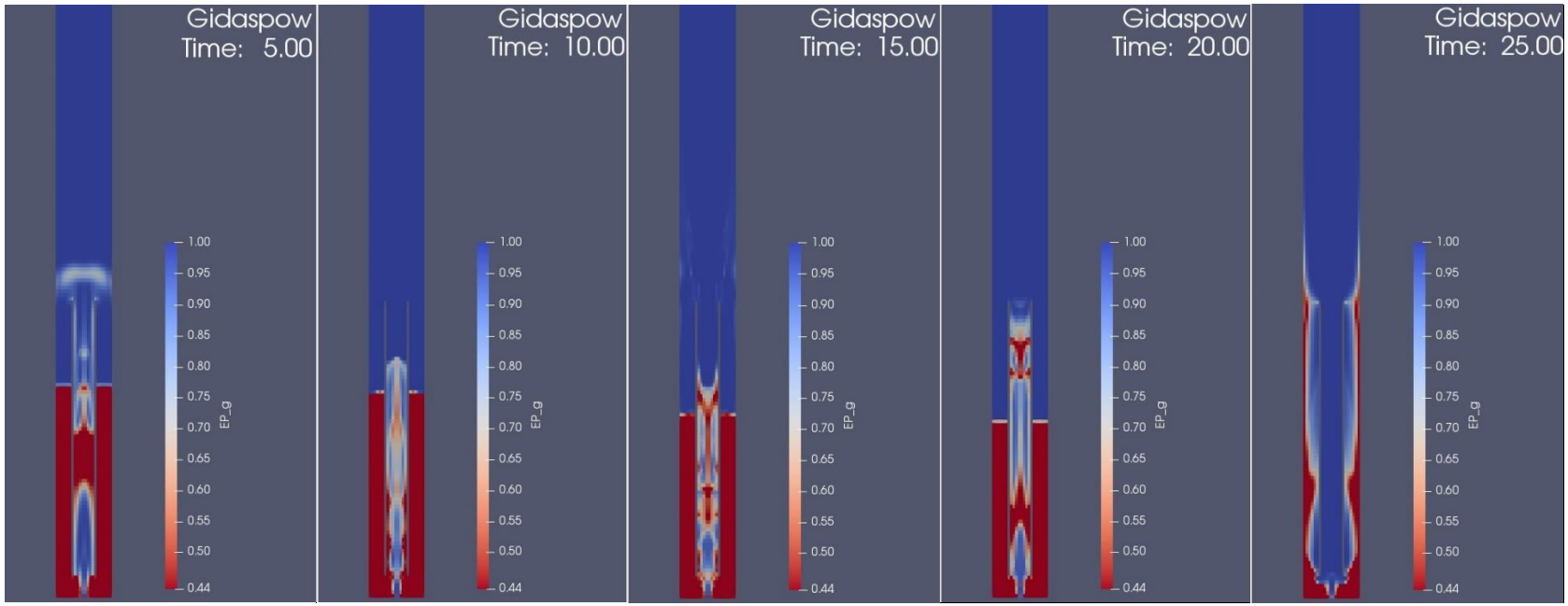

Figure 14. Gidaspow drag law gas void fractions at 5 sec incremental elapsed simulation time

From the results of the average pressure data and the visualization of the gas void fractions it may be concluded that the ideal drag law for our computational model is the Syamlal O'Brien with C1 D1 defined. The Wen-Yu model only gave an accurate representation of flow for under 10 seconds and the Gidaspow for 25 seconds while the C1 D1 define model remained stable over the entire time. Therefore, all simulations moving forward will utilize this drag law while completing their comparisons.

2.4 Geometry Coordinates Comparison

During the creation of the computational model in MFiX, you can define the coordinate system for your simulation. The two available coordinate systems are the cylindrical coordinate system and the Cartesian system. Coordinate system selection will have a significant impact on the computational cost of your model.

When selecting the cylindrical coordinate system in MFiX, a general assumption is that the bed has axisymmetric behavior. This assumption leads to a reduction in overall computational cost of the model as only half of the bed must be simulated. The asymmetric assumption has been studied in bubbling fluidized beds (41) and was found to be valid. Furthermore, the MFiX models that accurately depicted the laboratory spouted behavior in the previous research at UND utilized cylindrical coordinates further supporting the axisymmetric assumption.

If the Cartesian coordinate system is selected in MFiX, the entire bed geometry is simulated as a 2-D plane leading to increases in computational cost compared to cylindrical coordinates. The Cartesian system has been extensively studied in literature. Xie et al. (42) compared the performance of 2-D Cartesian to 2-D and 3-D cylindrical coordinates in fluidized beds of both cylindrical and rectangular bed geometries. They concluded that for bubbling fluidization there is reasonable agreement between all cases however as they increased gas velocities into new

fluidization regimes the models were no longer in agreement. This led them to suggesting to exercise cause when applying 2-D Cartesian coordinates to non-bubbling fluidization.

For our MFiX model we wanted to determine what effect changing the coordinate system had on the behavior of the model. The base cylindrical model used was the Syamlal O'Brien C1 D1 model from the drag law comparison. This model was then converted into Cartesian coordinates.

Similar to the drag law comparison, the average pressure in the spout region for the simulation time of 5-20 seconds was used to compare pressure profiles. The results of the average pressures may be seen in Figure 15.

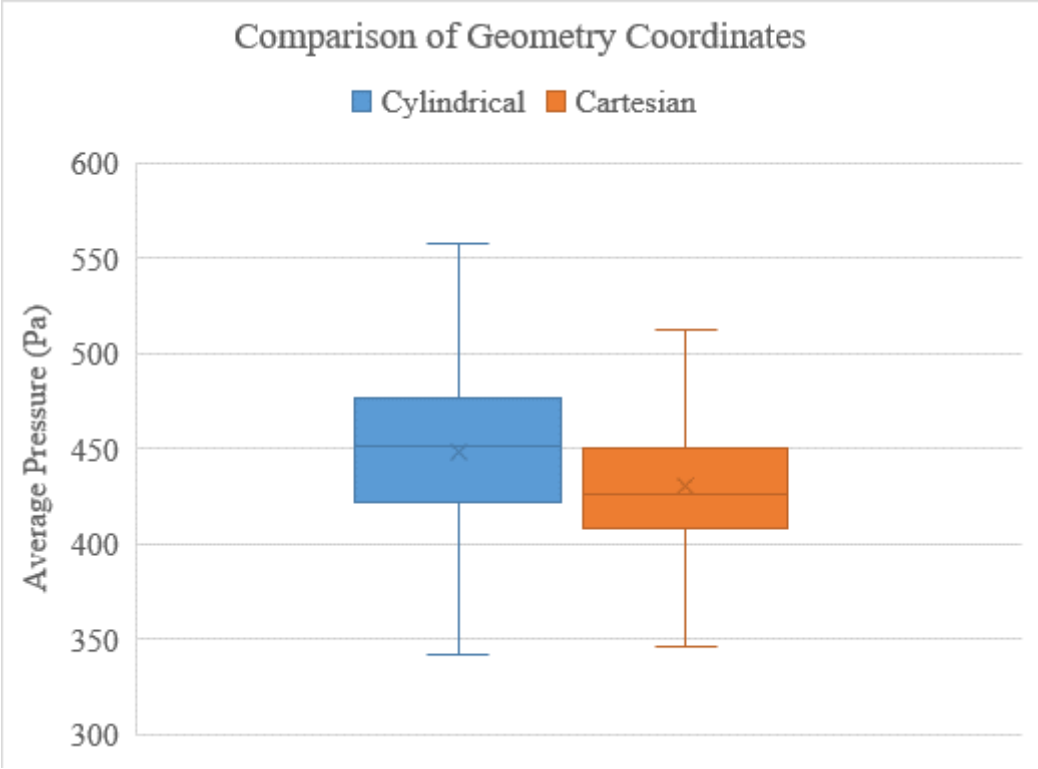

Figure 15. Comparison of average pressure in different geometry coordinates

The results of the pressure comparison show nearly identical average pressures for both coordinate systems, 449 Pa for cylindrical and 430 Pa for Cartesian. In addition, both coordinate

systems have no variance of their pressure values indicting stable spout flow into the draft tube section for both systems. However, if the gas void fractions of the beds are observed substantial differences in the behavior of the bed become apparent.

Figures 16-17 below compare the gas void fraction of the bed of both coordinate systems from the simulation range of 5-20 seconds.

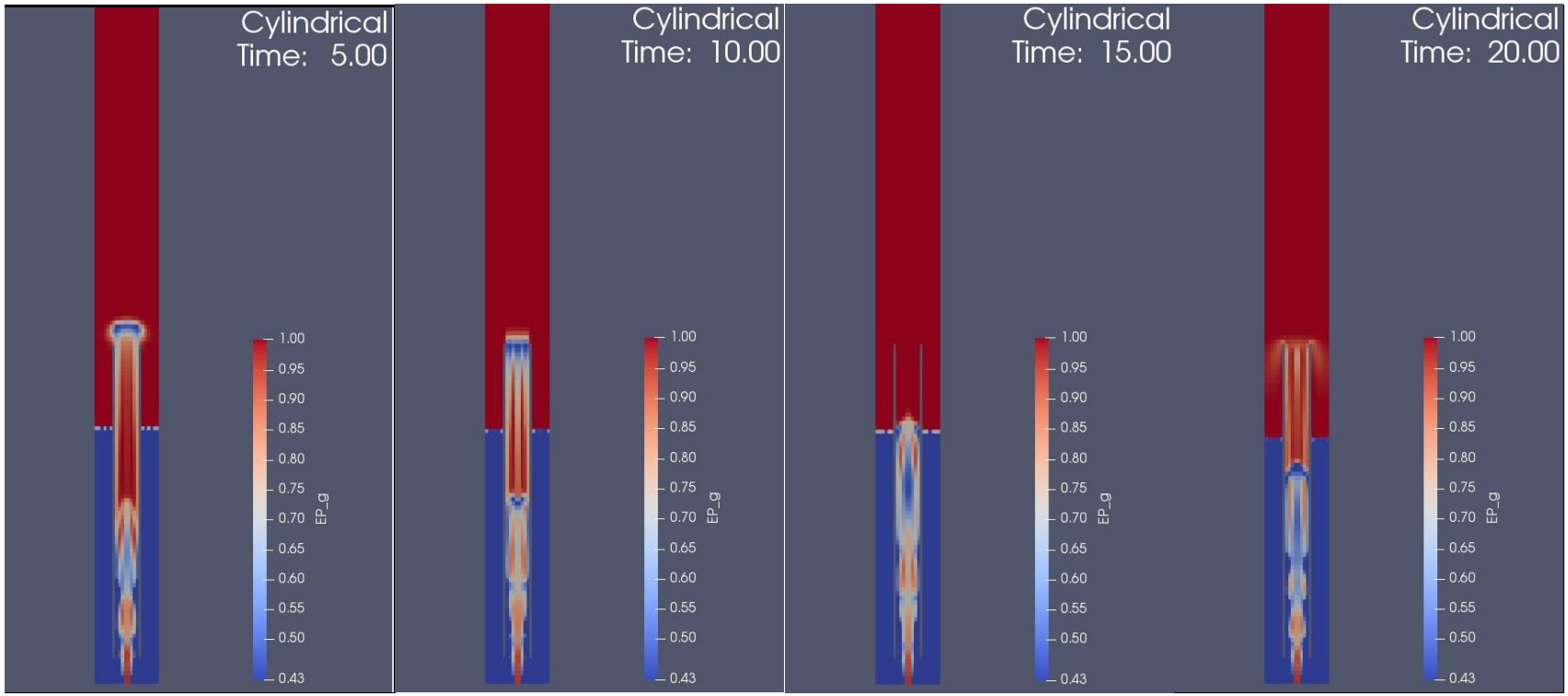

Figure 16. Cylindrical co-ordinate system gas void fractions at 5 second incremental elapsed simulation times

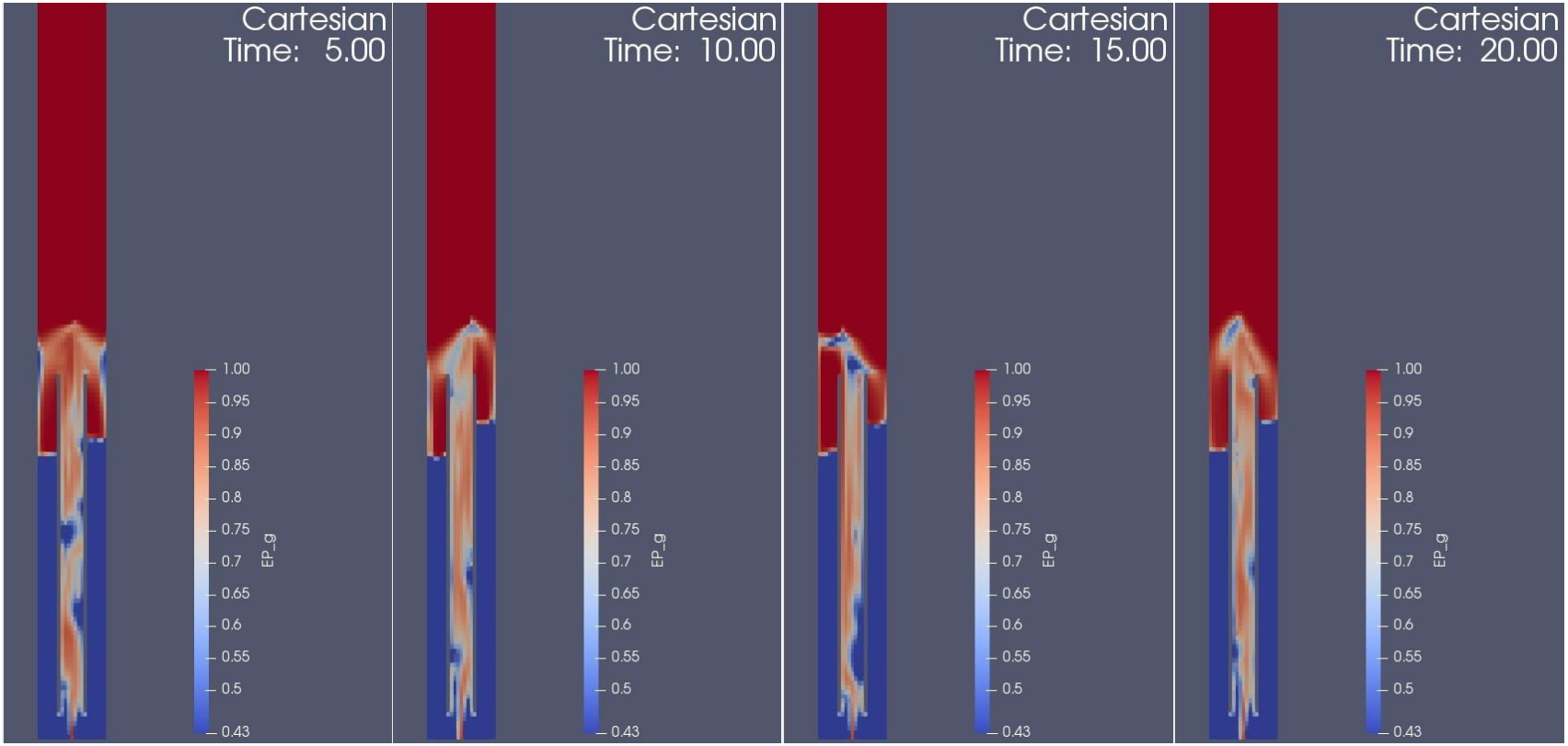

Figure 17. Cartesian co-ordinate system gas void fractions at 5 second incremental elapsed simulation times

Immediately at the 5 second simulation time, the coordinate systems are showing differing bed behavior. As described in previous sections, the bed behavior of the cylindrical coordinate system is intermittent spouting. The spouting behavior predicted by Cartesian coordinate system varies significantly.

When the Cartesian coordinate system is specified, the model predicts the bed to exhibit constant spouting with substantial variability in flow. At the various time steps, large clusters of solids are seen leaving the spout not in a uniform fountain like predicted in cylindrical model and observed in previous work at UND. Differences in the bed height in each of the coordinate system models can also be observed. The cylindrical model predicts a stable bed height across both annular regions while the Cartesian predicts two different bed heights due to the random distribution of solids from the unstable spout.

Based on the results of observing the gas void fractions of the two coordinate systems it can be concluded that the Cartesian coordinate system is not applicable for our spouted-fluidized bed MFiX model. The Cartesian model predicted significantly different behaviors from the cylindrical model which had been previous confirmed to accurately predict the behaviors of a laboratory scale reactor at UND. Therefore, going forward with the development of MFiX models for spout-fluidized beds the cylindrical coordinate system will be solely used.

2.5 Comparisons of Grid Size

The final MFiX simulation parameter studied was the effect of changing the grid size or resolution of the model. This is a common step in any CFD simulation to determine the grid independence of your model. The grid independence is defined as the point at which changing the grid size has no impact on the simulation result. Grid independence is a significant factor in CFD because the larger the grid size required for independence, the higher the computational cost.

One of the earliest examples of a grid independence study in MFiX was performed by Syamlal and Guenther (43). Their experiments concluded when they doubled the grid size of their model, they noticed a slight increase in diameter of the bubble in their fluidized bed. However, when they doubled the grid size again, they noticed no changes in bubble indicting the initial double grid size is sufficient to provide accurate results.

In our grid size comparisons, the optimized MFiX model from the comparisons of drag laws and coordinate systems was utilized to determine its grid independence. The initial grid size of the model was 11 x 240, 11 cells in I-direction and 240 cells in the j-direction. For our grid independence study, only the case of doubling the grid size to 21 x 480 was examined as further increasing the number of cells to 31 x 720 caused the simulation to fail. Following the same analysis as the comparisons of drag laws and coordinate systems, both the average pressures and gas void fractions of the bed for the two different grid sizes were studied.

Figure 18 displays the average pressure profiles of both grid sizes over the simulation time of 5-25 seconds. By increasing the grid size, the model predicts a lower pressure in the spout region of the draft tube. In addition, the range of average pressure values for the double grid size decreased indicting better stability of the spout region.

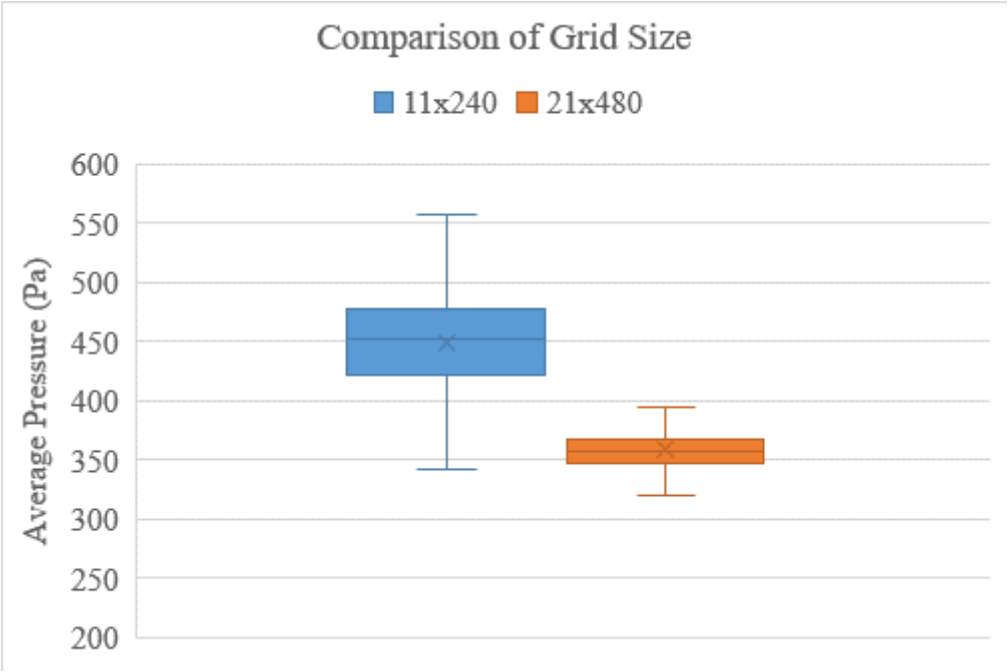

Figure 18. Comparison of average pressure in different grid size simulations

Matching the previous comparisons, the impact that the grid size has on physical behavior of the bed was determined by visualizing the gas void fractions of the MFiX model. The results of the gas void fractions at the simulation times 5-25 seconds, are displayed in Figures 19-20.

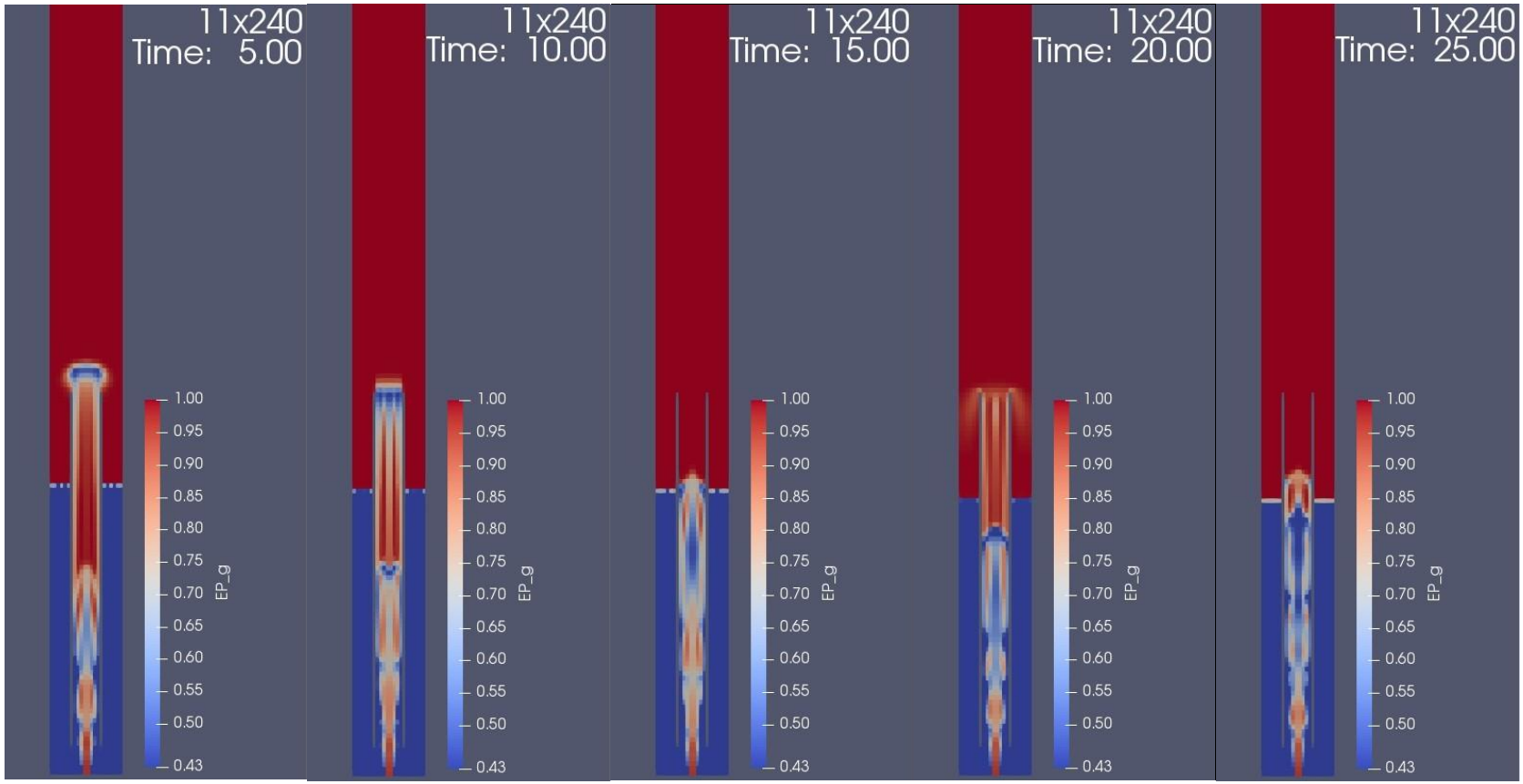

Figure 19. 11 x 240 grid size gas void fractions at 5 second incremental elapsed simulation times

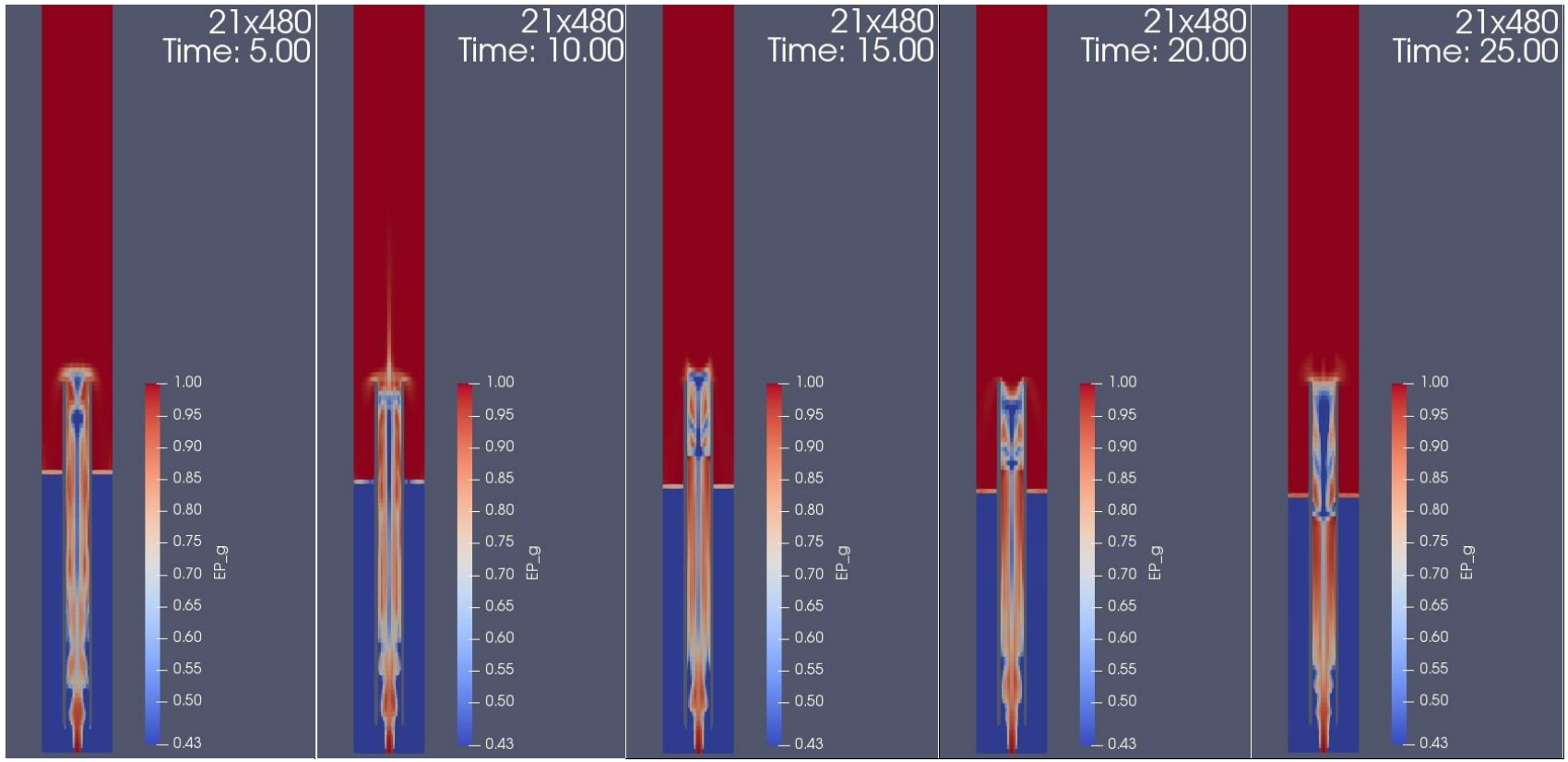

Figure 20. 21 x 480 grid size gas void fractions at 5 second incremental elapsed simulation time.

Over the 5-25 second simulation time visualized through the figures above, the bed is exhibiting different physical behaviors between the two grid sizes. Initially at the 5 second simulation time, both grid size models are predicting a spouting out of the draft tube. However, the 21x480 grid size also shows a large cluster of particles near the top of the draft tube ready to be spouted, while the 11x240 shows the particles are still cluster near the bottom of the draft tube. This behavior continues as the simulation progresses through the remaining time steps.

Each grid size model is displaying intermittent bed spouting behavior although more frequent spouting is observed in the 21x480 model. More frequent spouting occurs as the particles are concentrated higher in the draft tube and therefore require less force or energy to be removed. In the 11x240 model, the particles are concentrated lower in the draft tube, requiring greater forces to be exerted on the particles to spout them through the draft tube resulting in less frequent spouting.

Since the average pressure readings and bed void fractions are showing differing behavior between beds at the grid sizes, it may be concluded that we did not reach grid independence with the grid sizes chosen. As mentioned previously, a further increase of grid size from 21x480 to 31x720 caused the simulation to fail. Therefore, future work should be focused on confirming the results of the 21x480 model or creating a stable simulation of larger grid size to determine the models grid independence.

CHAPTER 3

SPOUTED FLUIDIZED BED DENSITY SEPARATION

3.1 Problem Overview

The second objective of this work was to determine if the computational modeling methods learned for the studies in Chapter 2 be applied to other advanced energy applications specifically with spouted fluidized beds. The energy application chosen was the separation of material based upon density and particle size. A spouted fluidized bed is an ideal choice for this application as within the fountain region of the spout there exists a driving force for density and particle size separation.

Kutluoglue et al. (44) examined the segregation of four types of spherical particles with densities ranging for 980-2,890 kg/m^3 and particle sizes of 1.1-2.2 mm. His results concluded that the light particles deflect more into the annular regions due to the collisions in the fountain with the heavier particles and the gas velocity profile of the spout. However, he also noted that while separation may be observed in the fountain, the annulus and spout regions promoted remixing and desegregation of the particles.

Research conducted by San Jose (11) agreed with the results of Kutluoglue. In their experiments they tested the effect of particle density on the separation of 3mm sized particles in a conical bottom reactor. San Jose concluded that the separation occurred as the lighter particles we concentrated near the sides of the reactor will the denser particles were concentrated near the

spout. Another important conclusion from their work was that the flowrate of the fluidizing gases and the spouting characteristics are key factors for density separation.

Additionally, Zhang et al (45,1) published two different studies on the effects of particle size and density in flat-bottom spout-fluid beds. Both studies were conducted on Geldart D particles like the work of San Jose and Kutluoglue. From the particle size experiments, they concluded that the size of the particle exerts a profound influence on the behavior of mixing and separation. Their results of the varying the density of particles agreed with San Jose, as they discovered as you varied the fluidizing gas into different flow regimes the separation behavior changes drastically. Interestingly, both the particle size and density experiments came to the same conclusions for separation in the spouting flow regime. In the spouting flow regime when the fountain is underdeveloped, the particle separation becomes extremely pronounced. Additionally, they observed that has the fountain becomes more pronounced, the degree of separation decreased.

3.2 Technical and Experimental Approach

The previous literature studies that have been completed on density separation have involved mainly Geldart D particles with conical bottom and flat bottom spout-fluid beds. Our approach was to use a spout-fluid bed with a draft tube similar in design to the beds in Chapter 2 and to focus on Geldart B particles. Specifically, the objective was to try and separate a particle mixture with a predefined concentration, by adjusting the design and fluidization settings of the bed.

CFD models for the spout-fluid bed with a draft tube were completed using ANSYS Workbench and ANSYS Fluent. ANSYS Workbench is the geometric design program where the physical parameters of the bed may be defined including the grid size. The Workbench design is

then uploaded into the CFD software, ANSYS Fluent, where the hydrodynamic parameters can be changed such as particle characteristics, fluidizing gas flows, and simulation drag laws.

The spout-fluid bed geometry that was built with the ANSYS software was a flat-bottom cylindrical spouted bed with a centralized draft tube. The initial key design and operational parameters were determined through the knowledge gained from the studies in Chapter 2 and background literature studies. Five main design factors were varied to determine the optimal design condition for bed stability and for separation to occur. The high and low levels of each of these factors are listed below in Table 7. In total 14 different simulations were run at the various design factors to determine the optimal design. A summary of the simulations and their design factor settings may be seen in Table 8.

Table 7. Design Factors for spouted bed draft tube geometry

Design Factor	Low	High	Units
Reactor Diameter	30.5	45.7	cm
Draft Tube Length	50.0	76.2	cm
Draft Tube Height from Spout	3.8	7.6	cm
Annulus Velocity	0	0.21	m/s
Spout Velocity	15	50	m/s

Table 8. Summary of simulations and design factor settings

Simulation Order	Reactor diameter (cm)	Draft Tube Height from Spout (cm)	Draft Tube Length (cm)	Annulus flowrate (m/s)	Spout flowrate (m/s)	Stable Spouting Achieved
1	30.5	3.8	76.2	0	35	No
2	30.5	3.8	76.2	0	40	No
3	30.5	3.8	76.2	0	50	No
4	30.5	7.6	76.2	0	35	No
5	30.5	7.6	76.2	0	40	No
6	30.5	7.6	76.2	0	50	No
7	45.7	7.6	76.2	0.21	50	No
8	45.7	3.8	76.2	0.21	50	No
9	45.7	3.8	50.0	0.21	30	No
10	45.7	3.8	50.0	0.21	20	No
11	45.7	3.8	50.0	0.21	15	No
12	**30.5**	**3.8**	**50.0**	**0.04**	**15**	**Yes**
13	**30.5**	**3.8**	**50.0**	**0.14**	**15**	**Yes**
14	**30.5**	**3.8**	**76.2**	**0.14**	**15**	**Yes**

-Bolded simulation indict where the most stable spouting behavior of the bed was achieved

In addition to the design factors that were varied, other important design and simulation variables still needed to be defined. Table 9 shows the inputs for those variables. The geometry design variables spout diameter, draft tube diameter, and bed height were all held constant throughout all simulations. In the simulation, ambient air was used as the fluidizing gas and defined as phase-1. Phase-2 was a lower density particle that had a larger particle size and was more abundant in the particle mixture. Phase-3 was a higher density particle but was present in the mixture at lower particle sizes and volume fractions.

Table 9. Fluent CFD model important design and simulation variables

Variable	Value
Reactor Length	305 cm
Spout Diameter	1.8 cm
Draft Tube Inner Diameter	5.7 cm
Draft Tube Thickness	0.3 cm
Bed Height	40 cm
Coordinate System	Cylindrical
Drag Model	Syamlal O'Brien C1 D1
Fluidizing Gas (Phase-1)	Ambient Air
Phase-2 solid density	1200 kg/m^3
Phase-2 particle size	300 µm
Phase-2 initial volume fraction	0.6
Phase-3 solid density	4000 kg/m^3
Phase-3 particle size	100 µm
Phase-3 initial volume fraction	0.02

3.3 Results and Discussion

In total 14 different CFD simulations were completed at the various key design factors to determine the optimal geometry and operating parameters to promote separation of the particles. Simulation numbers 1-6 utilized high spout flowrates with zero flow in the annulus. These simulations resulted in a highly unstable bed with irregular spouting. Therefore, in the simulations moving forward an annulus gas velocity was added and the reactor diameter was increased to try and stabilize the bed behavior.

In simulations 7-8 the effect of changing the draft tube height from the spout was studied at high annulus and spout flowrates. In simulation 7 with the high draft tube height, gas was found to be bypassing the draft tube and entering the annulus causing significant bed disruptions. Meanwhile in simulation 8, the spout behavior was still unstable with a specified annulus flowrate and the spout was not traveling the entire length of the draft tube. Thus, it was concluded to first lower the spout flowrate, and draft tube length.

Next, simulations 9-11 were run to determine the effect of solely changing the spout flowrate of the system. In each of the simulations, material traveled through the spout on the initial fluidization however in the preceding time steps material failed to travel the length of the draft tube. A conclusion on why this may be happening, is the high annulus flow rate is fluidizing the annular region with a greater force then the spout is providing. To combat this effect in the future simulations, the annulus flowrate and reactor diameter were decreased to reduce the potential for over-fluidization of the annular region.

Simulation 12 was conducted at the low value for most of the key design factors however a small annulus flow rate was added. Finally, the model predicted stable spouting behavior. However, the model failed to show any separation of the phases. When the volume fractions of the phases are observed, the values of the annular region are equal to their initial values indicting no separation occurred. For separation to be observed the resulting volume fractions should increase from the input which were their well-mixed void fractions. The resulting volume fraction of phase-2 and phase-3 can be seen on Figure.

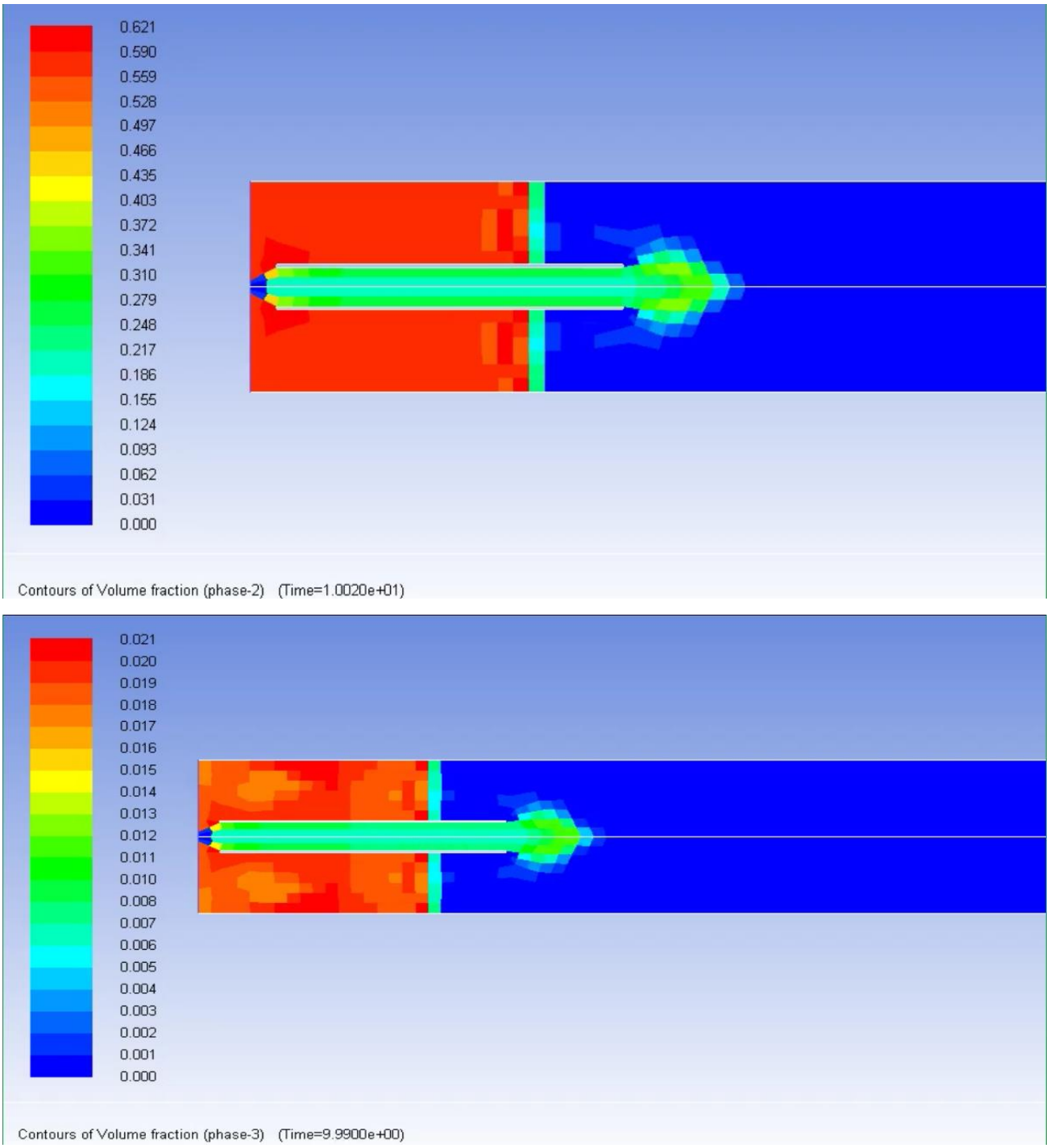

Figure 21. Simulation 12 volume fractions of phase-2 and phase-3 at 10 seconds elapsed simulation time

Simulation 13 was completed next to determine if increasing the annulus flowrate would facilitate the separation of the particles. The spout flowrate was held constant while the annulus

flowrate was increased from 0.04 m/s to 0.14 m/s. This resulted in a large change in the bed height of the particles which expanded past the draft tube, see Figure 31. No separation was observed as the bed was undergoing rigorous mixing in annulus due to the high flowrate. In the final simulation, the draft tube length was increased to prevent the annulus reaching the top of the draft tube at the higher velocities.

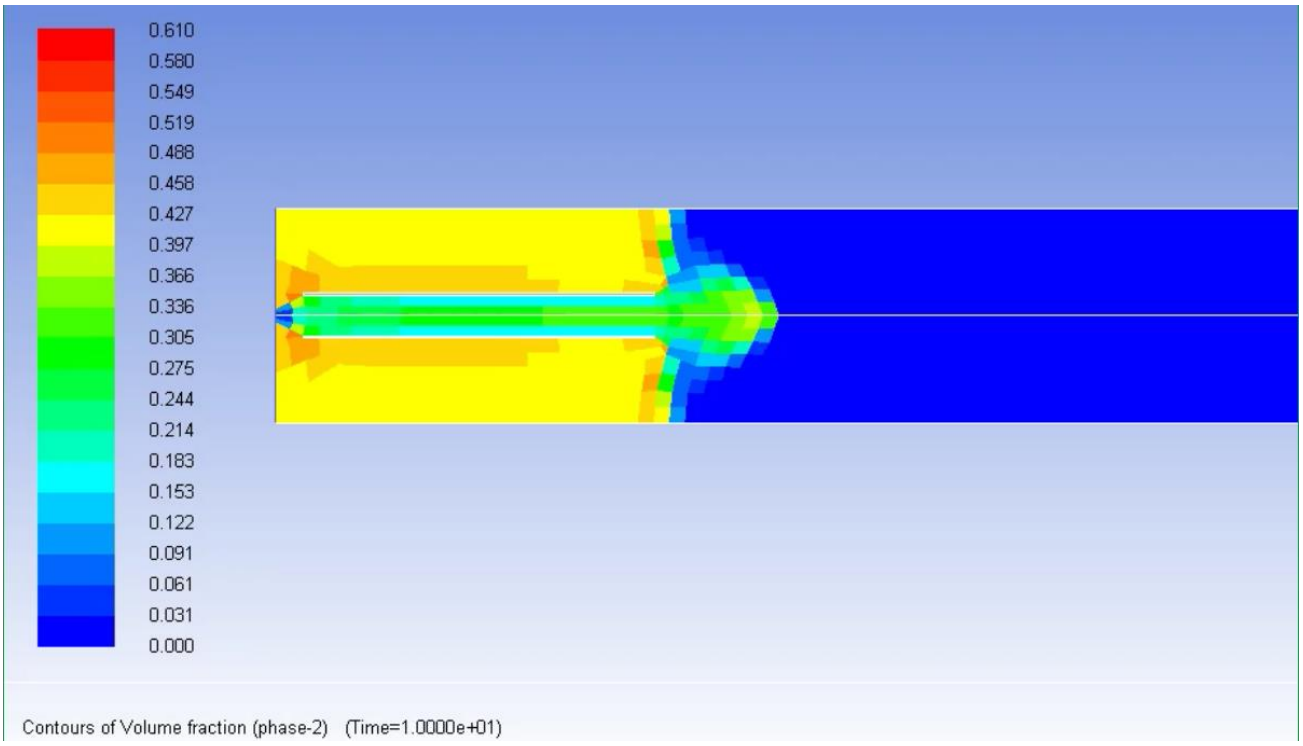

Figure 22. Simulation 13 volume fractions of phase-2 at 10 seconds elapsed simulation time

The final simulation ran, number 14, was similar to simulation 13 except the draft tube length was increased. It may be observed that the simulation produces a stable spout when observing the volume fractions of phase-2 and phase-3 in Figures 32. Additionally, it may be observed that phase-3 has an increased volume fraction near the walls in the annulus indicting they are fountaining towards the annulus. However, the value of volume of the fraction is only

improving by 5% from 0.021 to 0.022 which does not pronounce significant separation as it is a small change in relation to the overall solids volume fraction.

The failure of the simulations to achieve any separation of the particles may have been influenced by system limitations. For each of the particle phases, the particle size and density are held as constant factors. Therefore, the only the bed design parameters and operating conditions were altered to promote separation. Based on the results that none of the SFB simulations were able to predict any separation of the phases, a spout-fluidized bed would not be a recommended bed design when trying to separate particles based on density and particle size. The results of the simulations showed effective mixing of the two particles indicting potential for the bed design in applications such as coatings.

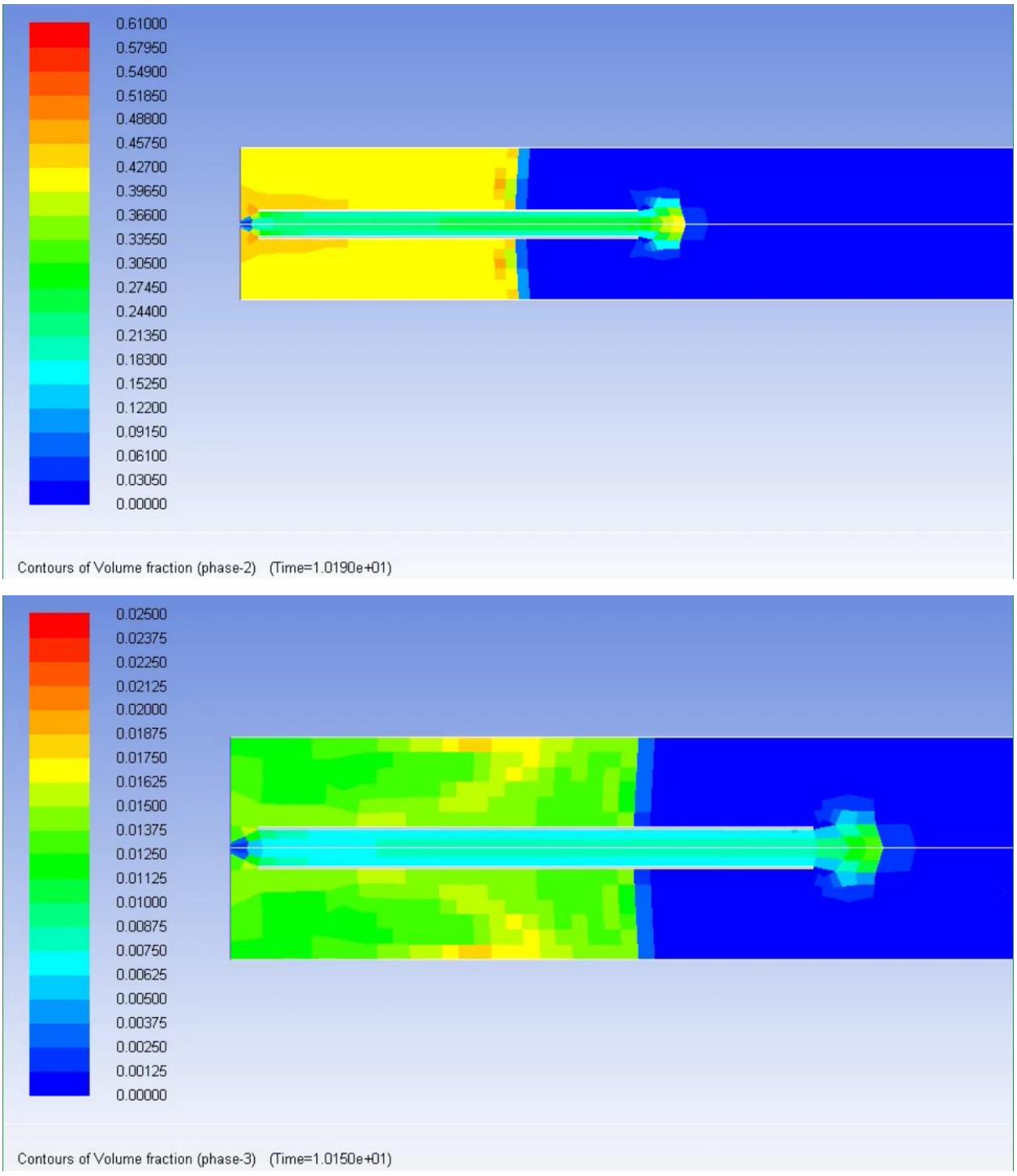

Figure 23. Simulation 14 volume fractions of phase-2 and phase-3 at 10 seconds elapsed simulation time

3.4 Density Based Separation Design Alterations

Since CFD simulations of flat-bottom SFB were not successful in achieving separation of particles, the design and operating parameters of conical spouted bed geometries were studied. Specifically, the goal of the study was to determine the effectiveness of the bed design to separate pyrite-rich minerals from coal. The success criteria for separation was defined as a product coal stream in which the dry-basis ash content was reduced from 38% to under 20%.

Unlike the flat-bottom simulations, an experimental conical spouted bed geometry existed and therefore CFD simulations and experimental testing occurred simultaneously. The conical spouted bed geometry created to study separation was designed using guidelines created by Epstein and Grace (22) as seen in Figure 24 while Table 10 defines the important design parameters from Epstein and Grace and includes the settings for the experimental geometry. The design also included sampling ports at various heights above the cone to allow for continuous sampling while operating. In total 19 trials were conducted using this experimental design.

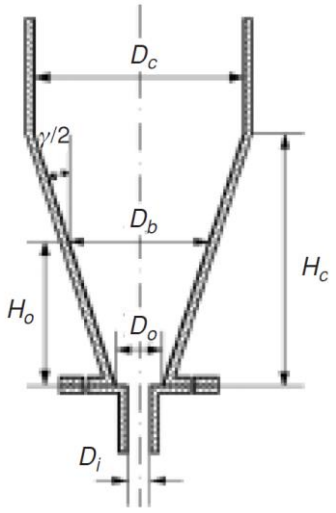

Figure 24. Geometry of conical spouted bed reactor defined by Epstein and Grace (22)

Table 10 Epstein/Grace design parameters for an experimental conical spouted bed

Design Parameter	**Epstein/Grace Descriptor**	**Bed Dimension**
Spout Tube Diameter	D_i	1/4 inch – 3/8 inch
Reactor Base Diameter	D_0	0.375 inch
Column Diameter	D_c	2 inches
Height of Cone	H_c	1.55 inches
Cone Angle	γ	55°

An ANSYS Fluent CFD model of the experimental geometry was designed to estimate the volume fraction of the coal during experimental trials. Results of the CFD models showed a stable spouting behavior of the bed as particles concentrated near the sides of the reactor while a small volume fraction was suspended in the spout region. In each trial the behavior predicted by CFD predicted similar behaviors seen during experimental testing. Therefore, it was concluded that CFD can give effective representations of the conical spouted bed geometry. Unfortunately, similar the flat-bottom CFD simulations the conical bed CFD simulations failed to create any significant separation. This conclusion is supported from the results of the experimental geometry.

From the 17 experimental trials of the conical spouted bed design, only two runs produced promising results. However, in each of these runs the total clean product coal collected was less than 5% of the original mass. Furthermore, the ash content of the clean product was 25-28% which is higher than the 20% ash content defined as the separation criteria concluding that no successful separation occurred.

CHAPTER 4

SUMMARY

4.1 Conclusions

With the work completed in Chapter 2 we were able to answer the key question proposed in the objectives section of Chapter 1. What design aspects of a spouted bed are shown to be significant using MFiX for CLC system? In previous work at UND, the physical design aspects of the spouted bed were studied, and the optimal values were found. These optimal values were then used in this work to identify the key hydrodynamic design aspects of the MFiX model not studied in previous work.

The first MFiX model parameter that was studied was the drag law defined for the simulation. Three different drag laws, Syamlal O'Brien C1 D1, Gidaspow, Wen-Yu, were simulated and their average pressures and gas void fractions were compared to determine any significant differences. The results showed that the Syamlal O'Brien C1 D1 was the only drag law that produced a stable bed over the simulation time and therefore was chosen as the ideal drag law in the proceeding simulations.

After the drag law comparison, the effects of specifying the coordinate system on the MFiX model was studied. The two coordinate systems compared were Cartesian and cylindrical coordinates with average pressure and gas void fractions being measured. It was concluded that the cylindrical coordinate system is ideal as it produced bed behaviors that agreed with experimental observations from previous work.

The final MFiX parameter studied was the effect of changing the grid size or resolution of the model to determine grid independence. Two different grid sizes were compared 11x240 and 21x480, any further increases in grid size caused the simulation to fail. Results of the grid size comparison showed differing bed behaviors between the grid sizes concluding that grid independence has not been established.

The objective of the work performed in Chapter 3 was use the knowledge gained about spouted fluidized beds with draft tubes from Chapter 2 and to design a bed that can achieve density separation of two different particles. The particle classification chosen, Geldart B, had not been commonly studied in literature.

In total 14 different simulations at varying SFB with a draft tube design conditions were completed. The results of one simulation case, determined the volume fraction of phase-3 increased by 5% however this increase is not enough to define significant separation. Additionally, other simulations displayed stable spouting behavior although all the simulations failed to show any degree of separation between the particles. Rather, the results of the simulations showed strong mixing between the particles. This agrees with observations of flat-bottom spout fluid beds of Geldart D particles from literature were separation was observed to be less pronounced in stable spouts in the spouting fluidization regime.

Additionally, an experimental design of a conical bottom spouted fluidized bed was created to determine if separation was achievable with a different geometry. CFD simulation results of the bed geometry agreed with experimental observations indicting the CFD model provided an accurate representation of the bed behavior of the physical model. Additionally, 17 experimental trials were conducted on the bed to determine ideal operating conditions to promote separation.

However, both the results of the CFD simulations and the experimental trials concluded that no significant separation occurred.

4.2 Future Work

A main objective for future studies of the MFiX model from Chapter 2 would be to apply the design methods to advanced geometries. Another common design for spout-fluidized beds includes a conical bottom to the geometry compared to the flat-bottom geometry in our studies. Comparisons could then be made between conical geometries with without draft tubes to define their flow characteristics and identify any potential uses in industry.

The main conclusion from the density separation work was that a spouted fluidized bed with a draft tube and a conical spouted bed would not work for the separation of Geldart B particles. Literature studies suggested separation may be more pronounced in spouting when the fountain is less pronounced. Therefore, future studies should focus on fluidized bed designs such as pulsed-bed systems with lower flowrates and particle circulation.

REFERENCES

1. US Department of Commerce, N. (2005, October 01). Global Monitoring Laboratory - Carbon Cycle Greenhouse Gases. Retrieved July 17, 2020, from http://www.esrl.noaa.gov/gmd/ccgg/trends/
2. World Energy Council. (2016). World Energy Resources 2016. Retrieved 2020, from https://www.worldenergy.org/assets/images/imported/2016/10/World-Energy-Resources-Full-report-2016.10.03.pdf
3. Hansen, J., Kharecha, P., Sato, M., et al. (2013). Assessing "Dangerous Climate Change": Required Reduction of Carbon Emissions to Protect Young People, Future Generations and Nature. Retrieved 2020, from http://journals.plos.org/plosone/article?id=10.1371%2Fjournal.pone.0081648
4. International Energy Agency. (2017). Renewables 2017: Analysis and Forecasts to 2022. Retrieved 2020, from https://iea.blob.core.windows.net/assets/ada7bd03-13ba-4f86-a92f-5f89935b6a2e/Renewables2017ExecutiveSummary.PDF
5. Black, J. (2013). *Cost and Performance Baseline for Fossil Energy Plants Volume 1: Bituminous Coal and Natural Gas to Electricity* (Rep. No. DOE/NETL-2010/1397). NETL.
6. Alvarez, R., Zavala-Araiza, D., Lyon, D., Allen, D., Barkley, Z., Brandt, A., . . . Hamburg, S. (2018, July 13). Assessment of methane emissions from the U.S. oil and gas supply chain. Retrieved 2020, from https://science.sciencemag.org/content/361/6398/186.full
7. IEA (2006), *Focus on Clean Coal*, IEA, Paris https://www.iea.org/reports/focus-on-clean-coal
8. NETL. (2020). Carbon Capture Program. Retrieved 2020, from https://netl.doe.gov/coal/carbon-capture
9. Yang, W. (2003). *Handbook of fluidization and fluid-particle systems* (p. 318). New York: M. Dekker.
10. NETL. (2020). COMPUTATIONAL DEVICE ENGINEERING TEAM-Facts Sheet. Retrieved 2020, from https://netl.doe.gov/sites/default/files/rdfactsheet/R-D222_1.pdf
11. San Jose, M.J., Alvarex, S., Garcia, I., Penas, F.J., *A Novel Technology to Segregate Binary Mixtures of Different Density in a Conical Spouted Bed*. The 14th International Conference on Fluidization – From Fundamentals to Products. 2013
12. Cocco, R., Karri, S. R., & Knowlton, T. (2014). Introduction to Fluidization. *Back to Basics*, 21-29. Retrieved 2020, from https://www.aiche.org/sites/default/files/cep/20141121.pdf
13. Kunii, D., & Levenspiel, O. (2012). *Fluidization engineering* (p. 39). Amsterdam: Elsevier.

14. Grace, J. (2009, March 26). Contacting modes and behaviour classification of gas-solid and other two-phase suspensions. Retrieved 2020, from https://onlinelibrary.wiley.com/doi/abs/10.1002/cjce.5450640301
15. Kunii, D., & Levenspiel, O. (2012). *Fluidization engineering* (p. 89). Amsterdam: Elsevier.
16. K. B. Mathur and P. E. Gishler. A study of the applications of the spouted bed technique to wheat drying. J. Appl. Chem., 5 (1955), 624–636.
17. Leva, M. (1959). *Fluidization*. New York, NY: McGraw-Hill.
18. Epstein, N., & Grace, J. R. (2011). *Spouted and spout-fluid beds: Fundamentals and applications* (p. 2). Cambridge: Cambridge University Press.
19. P. P. Chandnani and N. Epstein. Spoutability and spout destabilization of fine particles with a gas. In Fluidization V, ed. K. Østergaard and A. Sorensen (New York: Engineering Foundation,1986), pp. 233–240.
20. C. J. Lim, A. P.Watkinson, G. K. Khoe, S. Low, N. Epstein, and J. R. Grace. Spouted, fluidized and spout-fluid bed combustion of bituminous coals. Fuel, 67 (1988), 1211–1217.
21. Chatterjee, A. (1970). Spout-Fluid Bed Technique. *Industrial & Engineering Chemistry Process Design and Development, 9*(2), 340-341. doi:10.1021/i260034a032
22. Epstein, N., & Grace, J. R. (2011). *Spouted and spout-fluid beds: Fundamentals and applications* (p. 106). Cambridge: Cambridge University Press.
23. W. Q. Zhong and M. Y. Zhang. Pressure fluctuation frequency characteristics in a spout-fluid bed by modern ARM power spectrum analysis. Powder Technol., 152 (2005), 52–61.
24. W. Q. Zhong and M. Y. Zhang. Characterization of dynamic behavior of a spout-fluid bed with Shannon entropy analysis. Powder Technol., 159 (2005), 121–126.
25. Zhong, Wenqi & Chen, Xiaoping & Zhang, Mingyao. (2006). Hydrodynamic Characteristics of Spout-Fluid Bed: Pressure Drop and Minimum Spouting/Spout-Fluidizing Velocity. Chemical Engineering Journal - CHEM ENG J. 118. 37-46. 10.1016/j.cej.2006.01.008.
26. Fayed, M. E., & Otten, L. (1997). Chapter 11. In *Handbook of powder science & technology*. London: Chapman & Hall.
27. C. J. Lim, A. P.Watkinson, G. K. Khoe, S. Low, N. Epstein, and J. R. Grace. Spouted, fluidized and spout-fluid bed combustion of bituminous coals. Fuel, 67 (1988), 1211–1217.
28. D. O. Albina. Emissions from multiple-spouted and spout-fluid fluidized beds using rice husks as fuel. Renewable Energy, 31 (2006), 2152–2163.
29. M. S. J. Arnold, J. J. Gale, and M. K. Laughlin. The British Coal spouted fluidized bed gasification process. Can. J. Chem. Eng., 70 (1992), 991–997.
30. Yang WC, Keairns DL. Design of recirculating fluidized beds for commercial applications. AIChE Symposium Series 74(176):218–228, 1978a.
31. Altzibar, H., Lopez, G., Bilbao, J., & Olazar, M. (2013). Effect of draft tube geometry on pressure drop in draft tube conical spouted beds. *The Canadian Journal of Chemical Engineering*. doi:10.1002/cjce.21913

32. Yang, W. (2003). *Handbook of fluidization and fluid-particle systems* (p. 556). New York: M. Dekker.
33. Grbavčić, Z. B., Vuković, D. V., Jovanović, et al (1992). Fluid flow pattern and solids circulation rate in a liquid phase spout-fluid bed with draft tube. *The Canadian Journal of Chemical Engineering, 70*(5), 895-904. doi:10.1002/cjce.5450700510
34. Du, W., Bao, X., Xu, J., & Wei, W. (2006). Computational fluid dynamics (CFD) modeling of spouted bed: Assessment of drag coefficient correlations. *Chemical Engineering Science, 61*(5), 1401-1420. doi:10.1016/j.ces.2005.08.013
35. Gryczka, O., Heinrich, S., & Tomas, J. (2008). CFD-Modelling of the Fluid Dynamics in Spouted Beds. *Micro-Macro-interaction*, 265-275. doi:10.1007/978-3-540-85715-0_21
36. X.-L. Zhao, S.-Q. Li, G.-Q. Liu, Q. Song, and Q. Yao. Flow patterns of solids in a two-dimensional spouted bed with draft plates: PIV measurement and DEM simulations. *Powder Technology*., 183 (2008), 79–87.
37. R. G. Szafran and A. Kmiec. Periodic fluctuations of flow and porosity in spouted beds. *Transport in Porous Media*, 66 (2007), 187–200.

38. Watt, J. G., Laudal, D., et al. (2018). Development of a Spouted Bed Reactor for Chemical Looping Combustion. *Journal of Energy Resources Technology, 140*(11). doi:10.1115/1.4040403
39. Musser, J., & Carney, J. (2020). *Theoretical Review of the MFIX Fluid and Two-Fluid Models* (Tech. No. DOE/NETL-2020/2100). NETL. doi:10.2172/1604993
40. MFiX Documentation. (2020, August 14). Retrieved 2020, from https://mfix.netl.doe.gov/mfix/mfix-documentation/
41. Pain, C., Mansoorzadeh, S., Gomes, J., & Oliveira, C. D. (2002). A numerical investigation of bubbling gas–solid fluidized bed dynamics in 2-D geometries. *Powder Technology, 128*(1), 56-77. doi:10.1016/s0032-5910(02)00167-5
42. Xie, N., Battaglia, F., & Pannala, S. (2008). Effects of using two- versus three-dimensional computational modeling of fluidized beds. *Powder Technology, 182*(1), 1-13. doi:10.1016/j.powtec.2007.07.005
43. Guenther, C., & Syamlal, M. (2001). The effect of numerical diffusion on simulation of isolated bubbles in a gas–solid fluidized bed. *Powder Technology, 116*(2-3), 142-154. doi:10.1016/s0032-5910(00)00386-7
44. Kutluoglu, E., Grace, J. R., Murchie, K. W., & Cavanagh, P. H. (1983). Particle segregation in spouted beds. *The Canadian Journal of Chemical Engineering, 61*(3), 308-316. doi:10.1002/cjce.5450610309
45. Zhang, Y., Zhong, W., Jin, B., & Xiao, R. (2012). Mixing and Segregation Behavior in a Spout-Fluid Bed: Effect of Particle Size. *Industrial & Engineering Chemistry Research, 51*(43), 14247-14257. doi:10.1021/ie301005n
46. Zhang, Y., Zhong, W., Jin, B., & Xiao, R. (2013). Mixing and Segregation Behavior in a Spout-Fluid Bed: Effect of the Particle Density. *Industrial & Engineering Chemistry Research, 52*(15), 5489-5497. doi:10.1021/ie303577m